

**STREAMFLOW SIMULATION OF SATLUJ RIVER  
USING UBC WATERSHED MODEL**



जल है सब का जीवन

**NATIONAL INSTITUTE OF HYDROLOGY  
JAL VIGYAN BHAWAN  
ROORKEE - 247667**

1992-93

## PREFACE

There is no operational snowmelt runoff model in India while it is of prime importance for water resources management for all Himalayan rivers of India. One of the reason for limited studies carried out in this area is the non-availability of required data. Fortunately now for few snowbound catchments data is being collected and studies are being carried out.

In this study streamflows for Satluj river have been simulated using UBC watershed model. Simulations are made for three hydrologic years namely 1987/88, 1988/89 and 1989/90 at Rampur. The model has been calibrated. As a next step it is planned to test this model for snowmelt runoff forecasting in the same basin. This study has been carried out by Dr. Pratap Singh, Scientist 'B' during his visit to University of British Columbia, Vancouver, Canada under UNDP Project in the area of Snow Hydrology. He worked with Prof. M.C.Quick, Civil Engineering Dept. at UBC. The guidance of Prof.M.C.Quick is duly acknowledged. This report has been prepared by Dr. Pratap Singh, Scientist 'B', Mountain Hydrology Division, NIH, Roorkee.

*Satish Chandra*  
( SATISH CHANDRA )  
DIRECTOR

## CONTENTS

	PAGE NO.
<b>ABSTRACT</b>	i
<b>LIST OF FIGURES</b>	ii
<b>1.0 INTRODUCTION</b>	1
<b>2.0 STUDY AREA AND WEATHER SYSTEM</b>	4
<b>3.0 UBC WATERSHED MODEL</b>	8
3.1 Meteorological Data Distribution Algorithm	9
3.1.1 Temperature lapse rate	9
3.1.2 Precipitation elevation gradients	12
3.1.3 Orographic enhancement as a function of elevation and barrier height	13
3.1.4 Form of precipitation	14
3.1.5 Precipitation representation factors	14
3.1.6 Evaporation	15
3.2 Soil Moisture Model	16
3.2.1 First priority-fast runoff control	16
3.2.2 Second priority - Soil moisture and actual evapotranspiration	18
3.2.3 Third priority - Ground water percolation	18
3.2.4 Fourth priority - medium runoff	19
3.3 Watershed Routing	19
3.3.1 Fast runoff routing	20
3.3.2 Medium runoff routing	20
3.3.3 Slow runoff routing	21
3.4 Snowmelt Budget	21
3.4.1 Block budget	21
3.4.2 The wedge budget	21
3.5 Snowmelt and Simplified Energy Components	22

3.5.1	Shortwave radiation	24
3.5.2	Longwave radiation	25
3.5.3	Net longwave under cloudy conditions	26
3.5.4	Convective and advective heat transfer	27
3.5.5	Rainmelt	27
3.6	Application of simplified energy snowmelt equations	27
3.6.1	Cloud cover	28
3.6.2	Wind estimate	28
3.6.3	Albedo	28
3.7	Alternative Snowmelt Routine - UBC Degree-day Method	30
3.7.1	Forested melt formulation	31
3.7.2	Open-area melt formulation	31
3.7.3	Negative melt budget	32
3.8	Runoff from High Intensity Rain	32
4.0	<b>CALIBRATION OF MODEL</b>	35
5.0	<b>APPLICATION OF UBC WATERSHED MODEL TO SATLUJ RIVER</b>	40
6.0	<b>CONCLUSIONS</b>	57
	<b>REFERENCES</b>	59

## ABSTRACT

Streamflow simulation is carried out for the Satluj river in the western Himalayan region using the UBC Watershed Model. Snowmelt and glacier melt runoff constitutes the maor part of flow during spring and summers in this river. Daily simulation is made considering the whole watershed as a single unit and splitting it into two sub-basins. Streamflows are simulated for each sub-basin separately and total outflow is obtained by simply adding the flows. Superior results are obtained by dividing the watershed into two different sub-basins. The results confirm that combining two hydrological different watersheds into a single watershed reduces simulation or forecasting accuracy. A brief description of the UBC Watershed Model is also presented. It is reported that areal distribution of precipitation is the most important factor in the streamflow simulation because snowpack is built up by the model from observed precipitation and from precipitation-elevation relationships.

**LIST OF FIGURES**

<b>S.NO.</b>	<b>TITLE</b>	<b>PAGE NO.</b>
1.	Index map showing location of study watershed	2
2.	Area-elevation curve of the study method	5
3.	Mean monthly precipitation for stations in the watershed	6
4.	UBC watershed model - general flow chart	10
5.	Daily lapse rates as a function of daily temperature range	11
6.	Model of soil layer and subdivision of runoff components	17
7.	Variation in mean seasonal winter precipitation with elevation	37
8.	Mean monthly temperature lapse rates between Namgia and Kaza	37
9.(a)	Observed and simulated streamflows for the year 1987-88 considering watershed as a single unit	41
(b)	Observed and simulated streamflows for the year 1988-89 considering watershed as a single unit	42
(c)	Observed and simulated streamflows for the year 1989-90 considering watershed as a single unit	43
10.(a)	Observed and simulated streamflows for the year 1987-88 for the upper subbasin (Spiti)	45
(b)	Observed and simulated streamflows for the year 1988-89 for the upper subbasin (Spiti)	46
(c)	Observed and simulated streamflows for the	47

	year 1989-90 for the upper subbasin (Spiti)	
11.(a)	Observed and simulated streamflows for the year 1987-88 for the lower subbasin	48
	(b) Observed and simulated streamflows for the year 1988-89 for the lower subbasin	49
	(c) Observed and simulated streamflows for the year 1989-90 for the lower subbasin	50
12.(a)	Observed and simulated streamflows for the year 1987-88 by splitting watershed into two subbasins and combining the flows	51
	(b) Observed and simulated streamflows for the year 1988-89 by splitting watershed into two subbasins and combining the flows	52
	(c) Observed and simulated streamflows for the year 1989-90 by splitting watershed into two subbasins and combining the flows	53
13.	Build-up and depletion of snow water equivalent for the year 1988-89	54
14.	Changes in the albedo with season.	56

LIST OF TABLES

1.	Model efficiency ( $R^2$ ) for individual subbasins and total watershed	59
----	---	----



## 1.0 INTRODUCTION

The major river systems of Northern India, namely Indus, the Ganga, the Brahmaputra and their tributaries originate in the Himalayas and contribute a large part of the water resources of India. However, during the spring and summer period runoff is comprised mostly of snowmelt and is the source of water for irrigation, hydroelectric power and drinking water supply. It is estimated that 30-50% of the total annual water yield of these major rivers of Northern India is provided by the snow and glacier melt runoff (Agarwal et al, 1983). An accurate estimate of volume of water contained in snowpack and the rate of its release are therefore needed for efficient management of water resources, which includes flood forecasting, reservoir operation, design of hydrologic and hydraulic structures, etc. Investigations to understand the snowmelt processes and snowmelt forecasting techniques are required for proper utilization of abundant water resources available in the Himalayan region.

The present status of snowmelt studies in India shows that daily or seasonal snowmelt runoff forecasting have not been carried out and yet they are of prime importance for management of water resources (Singh, 1991). Only some efforts have been made to develop regression relationship between snow cover area and runoff (Ramamoorthi, 1986). This may be because only limited meteorological and streamflow data was available for Himalayan catchments, less than required for snowmelt forecasts. In recent years, the condition of data network has improved for several snowbound catchments and systematic and continuous efforts are being made to collect the required data. Satluj catchment is one of the catchments.

In the present study attempts have been made to simulate the streamflows in the Satluj catchment, using the UBC watershed model. The study is undertaken in the middle part of Satluj basin upto Rampur because the major contribution of snowmelt in the Satluj is from this part of the basin. The area under study is shown in Figure 1 and hereafter will be referred to as the study watershed. The daily flows are simulated for 3 consecutive hydrologic years, namely, 1987/88, 1988/89 and 1989/90, using a hydrologic year from October to September. The UBC watershed model is already operational for long term and short term forecasting in the Columbia, Peace and Fraser river systems in Canada covering basin areas from 1000 up to 10,000 sq.km. The model has the ability to continuously monitor the hydrologic state of the catchment over extended periods of time; and it maintains a consistent relationship between meteorological input and the

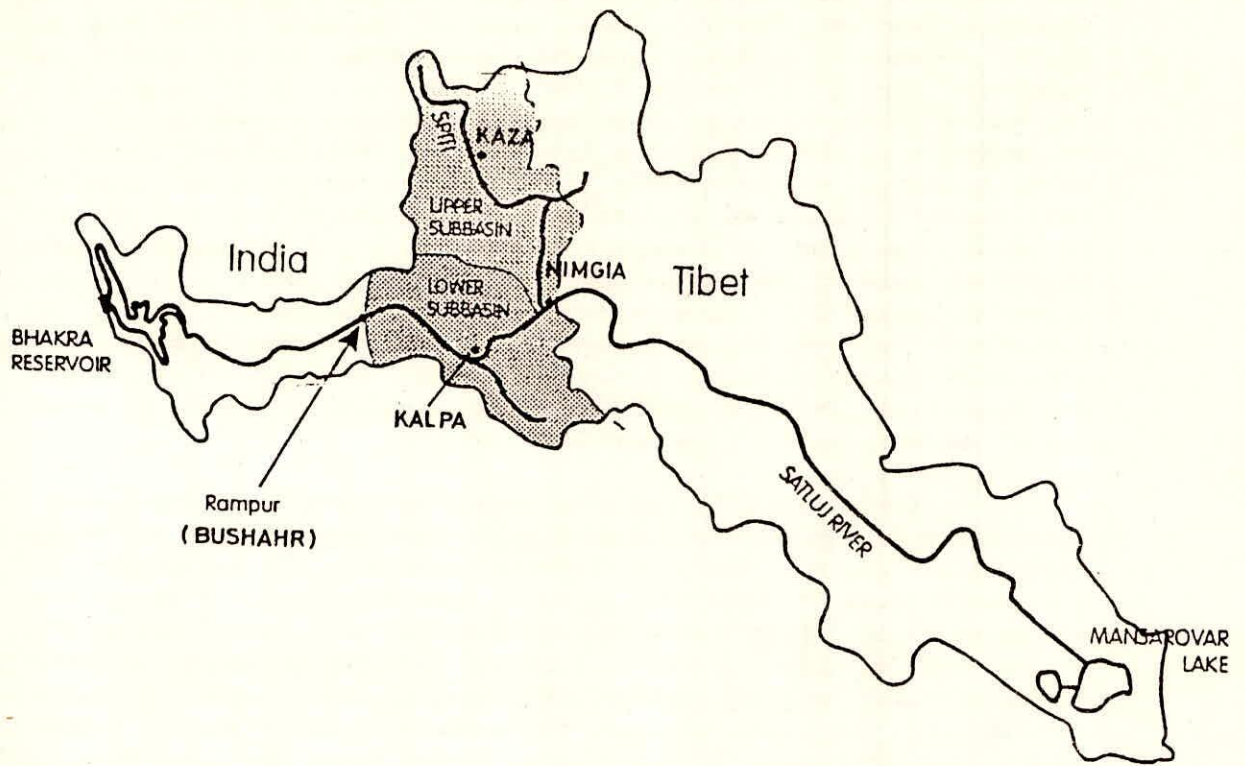


Figure 1. Index map showing location of study watershed (shaded area)

recorded basin runoff; both these abilities tend to substantiate the parametric interrelationship used in the model. The purpose of this study is to assess the performance of UBC watershed model for daily streamflow simulation in a watershed which experiences very uneven and nonsystematic precipitation distribution with drastic variation in relief and produces significant snowmelt runoff in the summer.

The river Satluj is one of the main tributaries of Indus and has its origin very near to the Indus headwaters. It rises in the lakes of Mansarovar and Rakastal in the Tibetan plateau at an elevation of about 4572 m. The total catchment area of Satluj is about 56130 sq.km of which 36075 sq.km lies in Tibet and the remaining about 20056 sq.km in India. The entire area in the Tibetan plateau and some areas in the downstream are mostly without rainfall and have a cold desert climate, and this results in low flow in the Satluj river until it joins its major tributary, Spiti, near Namgia in India. The Spiti watershed experiences extensive snowfall in the winters and therefore substantially contributes to the Satluj flows in the form of snowmelt runoff in the summer months. There are several other tributaries which join the Satluj river in the downstream and swell its flow. Only about 11% area of the total Satluj catchment is covered by glaciers (Upadhyay et al, 1983).

The area under study experiences snowfall in the winter season and very little rainfall in the summer. A major contribution from this area comes from the melting of snow and glaciers only. The elevation varies from 1500 m to 7026 m for this area, but very little area is above 5400 m. The area elevation curve is shown in Figure 2. The area-elevation curve suggests that only about 2.6% of the watershed area lies above 5400 m.

The main snowfall period in this catchment is from December to March and sometimes extending from October to April. The precipitation during winter occurs due to "western disturbances", the extra tropical disturbances moving from west to east originating from the Caspian and Mediterranean seas and moving across Iran, Afghanistan and Russia. Several western disturbances in the winter season move over Northern India with an average frequency of 5 to 6 disturbances in a month. The duration of individual storm varies from 1 to 7 days, generally being 2 days. Precipitation of 3 to 4 cm/hr is quite common (Rao, 1983). Generally maximum precipitation occurs in the month of March (Figure 3), whereas minimum precipitation is observed in the month of June. This figure also shows that the lower part of the watershed receives higher amount of precipitation in comparison to upper part of the watershed. The permanent snowline in this region of Himalayas is about 5400 m (BBMB, 1988).

The snowmelt contribution starts from about mid March and lasts until June/July depending upon the snowpack water

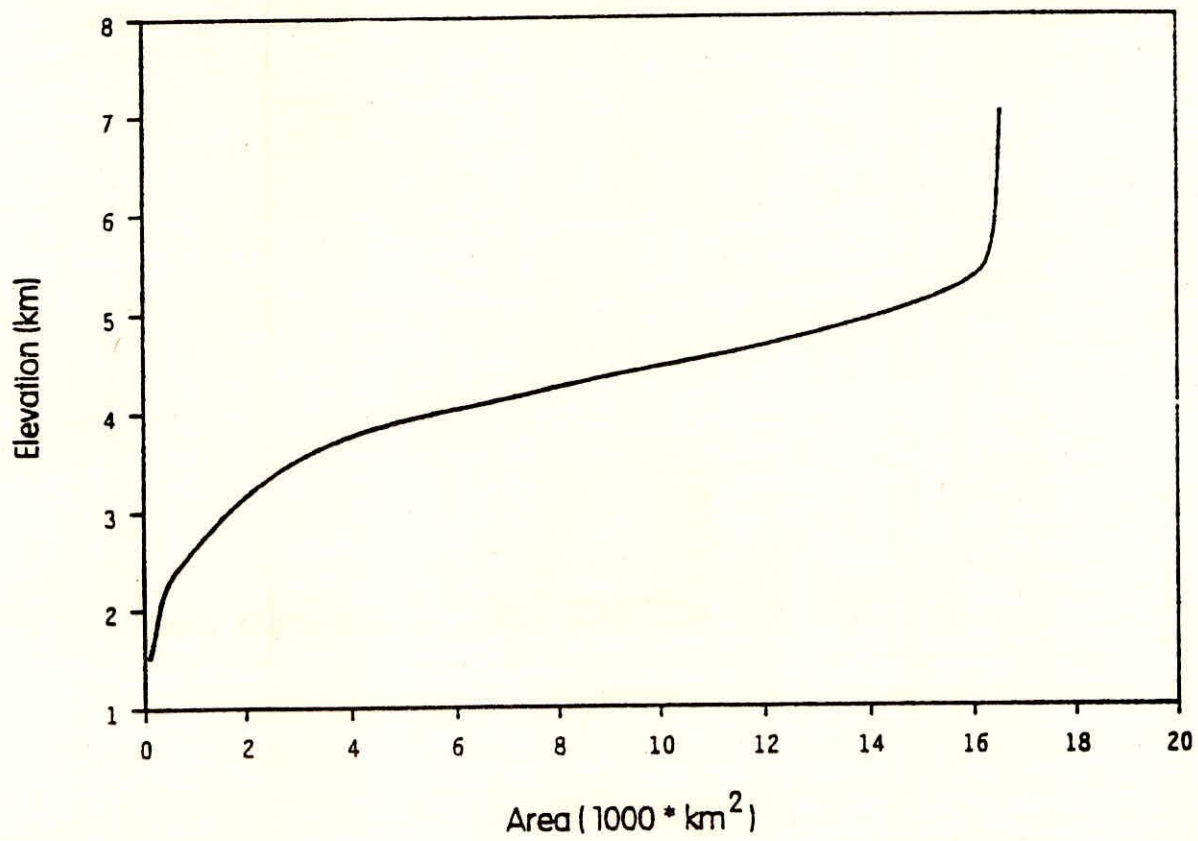


**Figure 2. Area-elevation curve for the study watershed**

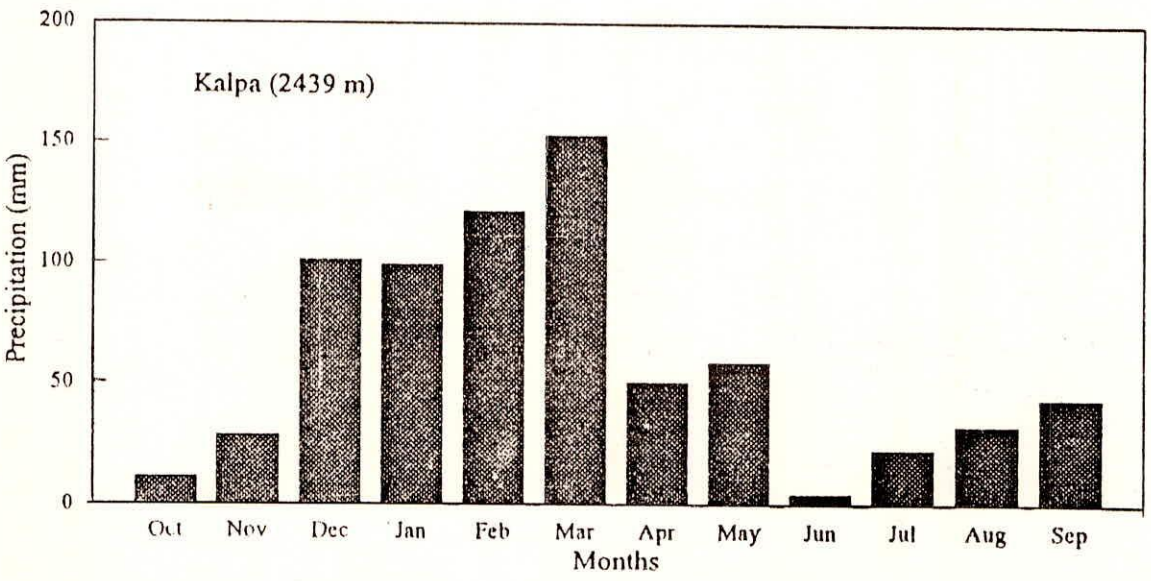
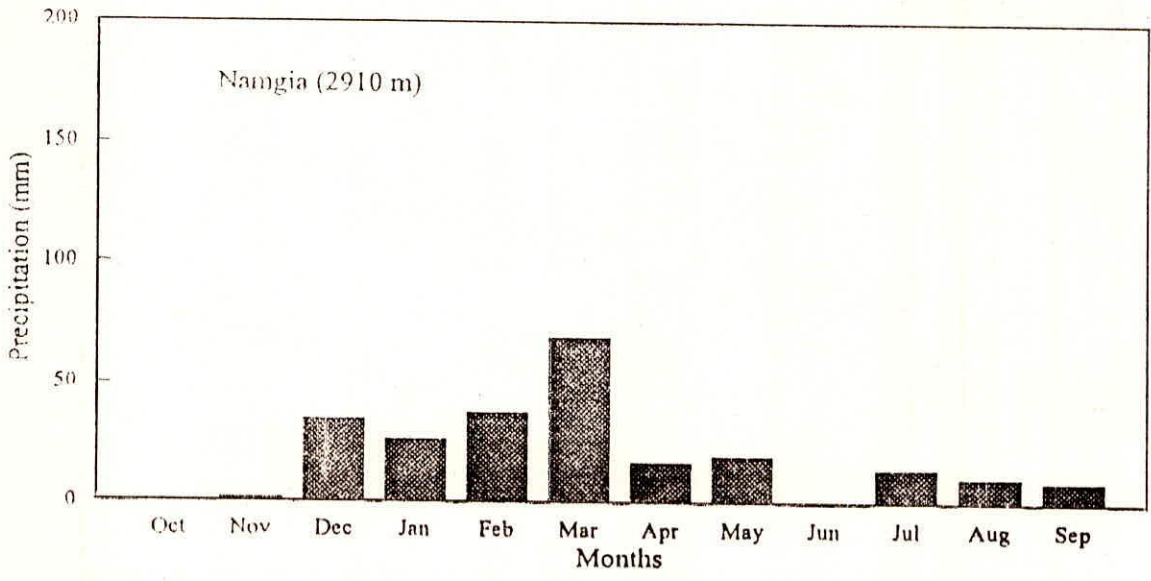
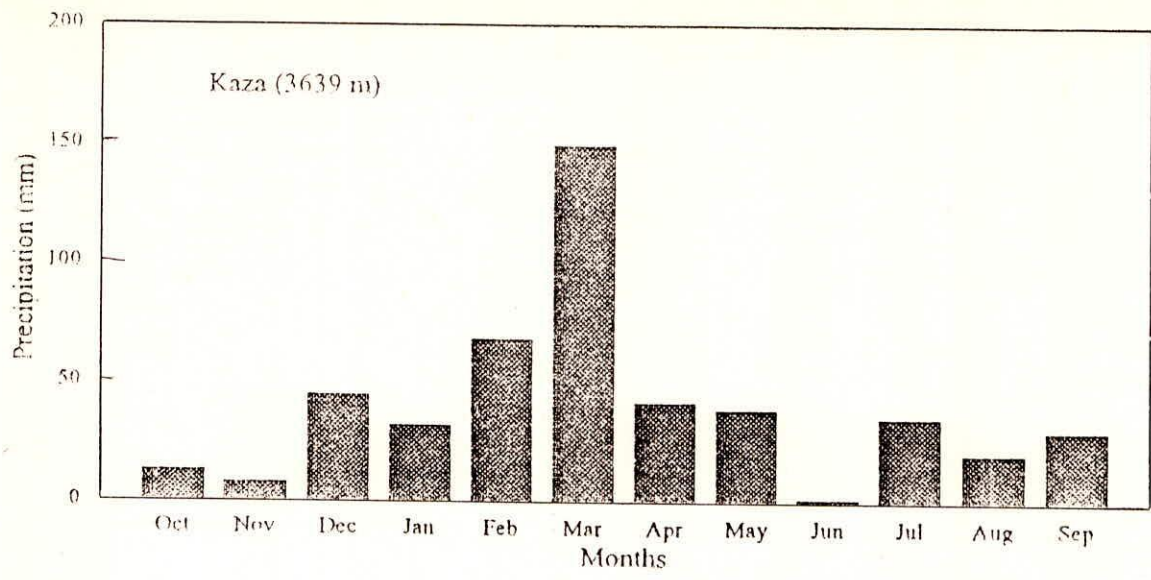


Figure 3. Mean monthly precipitation for the stations in the watershed

equivalent accumulated in the preceding winter season and prevailing temperature in the summer season. The glacier melt runoff in the months of July to September occurs after the contribution of seasonal snowmelt, when the glaciers become snow-free. Peak values of total discharge in July and August are essentially due to monsoon rains in the lower part of the basin.

### 3.0 UBC WATERSHED MODEL

The UBC watershed model has been developed by Quick and Pipes (1977) at the University of British Columbia (UBC), Canada. The watershed model is designed to give a computational representation of watershed behaviour. The input data requirements are daily values of maximum and minimum temperatures and precipitation. The model calculates on a daily basis the time distribution of streamflow leaving the catchment as a result of snowmelt and rainfall. In addition to this basic capability for calculating streamflow, the model also calculates and prints out the current moisture status of the watershed; in particular it calculates accumulation and depletion of snowpacks by elevation. Other aspects of this moisture budget status are soil moisture, evaporation, and the quantities of water in the various runoff storage systems. Given continuous meteorological input data, the model will operate continuously, accumulating and depleting snowpacks and producing estimates of daily streamflows. For calibration and streamflow as reference data and calculates performance statistics of volume and shape reconstitution.

The watershed model was designed primarily for short term river flow forecasting. The accuracy of this forecast depends on

- (a) the current assessment of the snowpacks and soil and groundwater storages,
- (b) the representativeness of the meteorological data to date, and
- (c) the accuracy of the meteorological forecast.

Because the watershed model operates continuously if given continuous meteorological input, it has been found possible to use the model for long term forecasting using assumed patterns of weather. This capability can be used to assess the range of possible outcomes for a whole season of snowmelt and rain runoff once an initial watershed status has been specified. Such seasonal forecasts can be upgraded with the recorded data as the season advances and the possible range of outcomes will gradually narrow. An extension of this mode of operation has been the use of the model to estimate complete years of data when the streamflow records have not existed, but for which meteorological data is available.

The following sections outline the various algorithms used to describe the processes involved in input data interpretation and generation of runoff due to snowmelt glacier



melt and rainfall. A general flow chart of the model is shown in figure 4.

### 3.1 Meteorological Data Distribution Algorithms

Meteorological data is available as point values at given elevations in a watershed. The model is designed to handle data from up to a maximum of three stations. Before watershed response calculations can be made, these meteorological data at a point must be distributed to the mid-elevation points of elevation bands.

#### 3.1.1 Temperature lapse rate

Lapse rates are known to be quite variable, ranging from high values of about the dry adiabatic lapse rate to low values representing inversion conditions. A complete and detailed representation of this lapse rate variability is not possible, but the main features of lapse rate can be represented as a function of daily temperature range.

The following major features of lapse rate variation are recognised in the temperature lapse rate algorithm:

1. During continuous rainstorm conditions the lapse rate will approximate the saturated adiabatic rate. Under these conditions the daily temperature range will tend to be zero or very low.
2. Under clear sky, dry weather conditions, the lapse rate during the warm part of the day will tend to the dry adiabatic rate. During the night, under these clear sky conditions, radiation cooling will cause the temperatures to fall to the dew point temperature, and this is particularly true for a moist airmass. As a result, night-time lapse rates under clear skies will tend to be quite low, and at times even zero lapse rates will occur.

Based on these considerations, two lapse rates are specified in the model, one for the maximum temperature and one for the minimum temperature. The lapse rate is calculated for each day using the daily temperature range (diurnal range) as an index. The functional relationships are shown in Figure 5. Their general form is given below.

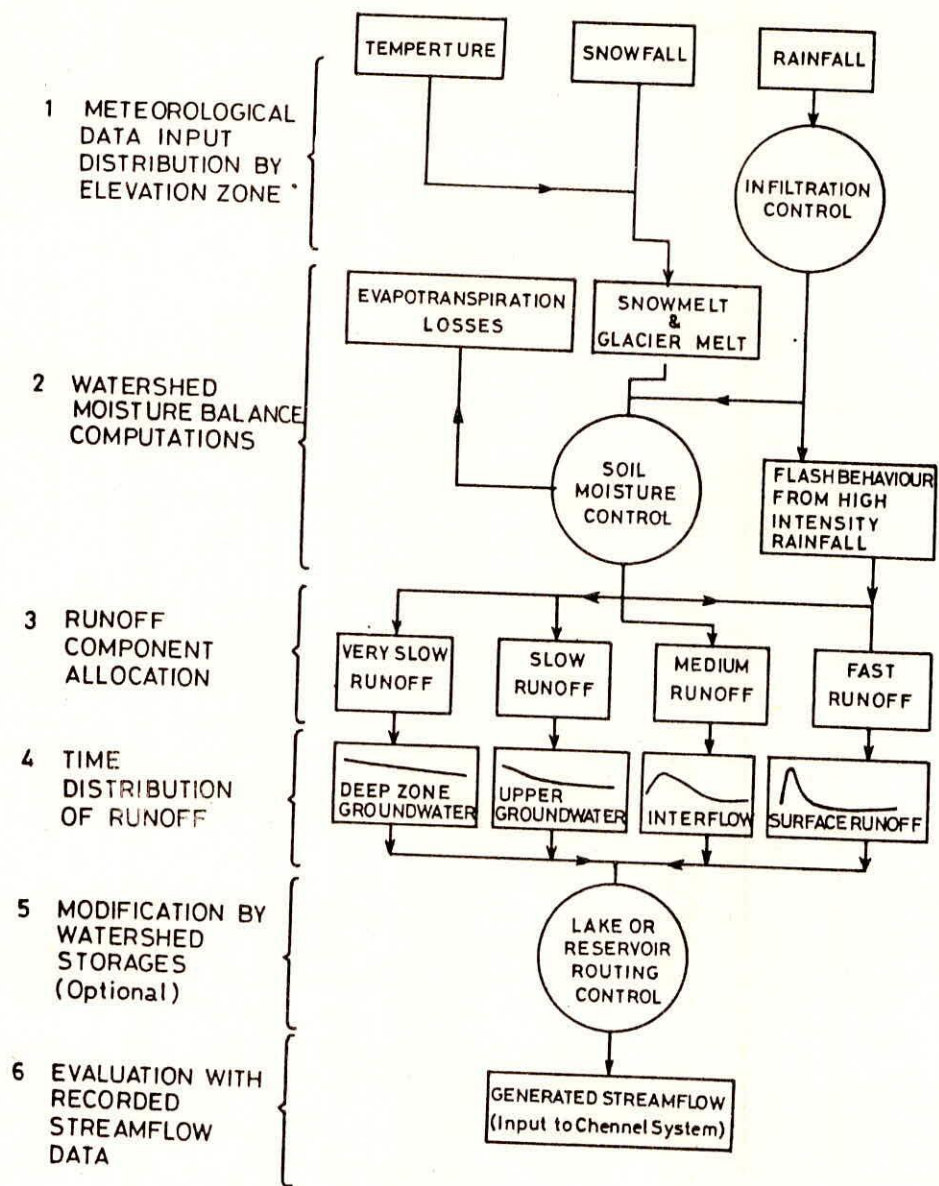
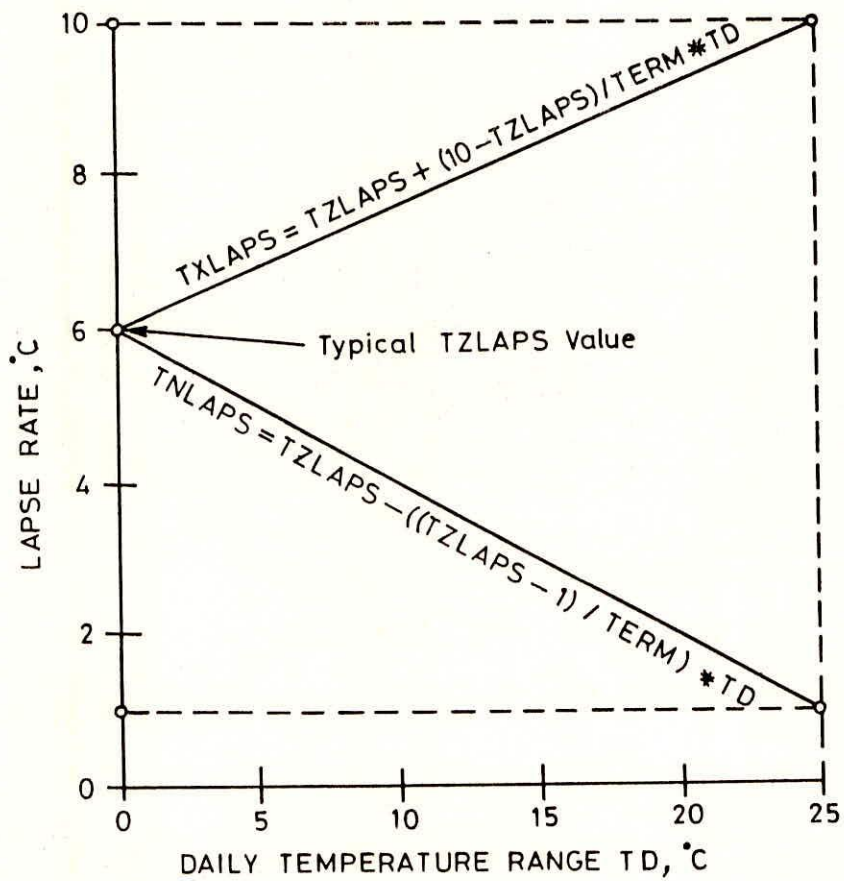


Fig. 4 UBC Watershed Model - General Flow Chart



(ASSUMES TERM = 25 °C, TLXM = 10 °C, TLNM = 1 °C)

Fig. 5 Daily Lapse Rates as a function of Daily Temperature Range.

Maximum Temperature Lapse rate - TXLAPS

$$\text{TXLAPS} = \text{TZLAPS} + (\text{TLXM} - \text{TZLAPS}) * \text{TD} / \text{TERM}$$

Minimum Temperature Lapse Rate - TNLAPS

$$\text{TNLAPS} = \text{TZLAPS} - (\text{TZLAPS} - \text{TLNM}) * \text{TD} / \text{TERM}$$

where

$$\text{TD} = \text{daily temperature range (TX-TN)}$$

and

$$\text{TZLAPS} = \text{TZ} - (\text{PP} / \text{PPM}) * (\text{TZ} - \text{TZP})$$

for the above,

- PP = daily precipitation
- TLXM = 10<sup>o</sup> C/km
- TLNM = 0.5<sup>o</sup> C/km
- TZ = 6.4<sup>o</sup> C/km, that is, a reference lapse rate for rain-free conditions
- TZP = 3.2<sup>o</sup> C/km, that is, a reference lapse rate when pp ≥ PPM
- PPM = 10 mm/day

and the calibration parameter TERM equals the maximum temperature range under open sky conditions (selected from the data set (TX-TN)).

### 3.1.2 Precipitation elevation gradients

The enhancement of precipitation as a moist air mass driven by wind across mountain barriers is an important aspect of mountain watershed modelling and is referred to as orographic precipitation.

Orographic precipitation is influenced by three main factors, the slope of the mountain side, the mountain barrier height and thirdly, the stability of the airmass. The generalize, the steeper the mountain side, the more rapid the increase in orographic precipitation. However, this increase in precipitation with elevation does not continue indefinitely, but tends to decrease substantially at about half the maximum mountain barrier height and shows no further increase above about two-thirds of the maximum mountain height.

The stability of the air mass depends on the relative values of the saturated adiabatic lapse rate and the prevailing lapse rate of the surrounding airmass. A useful index of stability can be developed by comparing the values of the saturated and dry adiabatic lapse rates. The saturated adiabatic lapse rate is dependent on temperature being considerably less than the dry adiabatic rate (Chow, 1964) when temperatures are high, but increasing to similar values as the dry adiabatic rate when temperatures are low. This variation of saturated adiabatic lapse rate will be used to account for the variation in orographic precipitation influences between winter snowfall, which is relatively insensitive to orographic effects.

The algorithms which describe the variation of precipitation with elevation are subdivided into two aspects to give the final orographic effect. The first algorithm describes the basic enhancement of precipitation with elevation barrier height if the temperature is 32°F and the second algorithm modifies that basic distribution for variations in temperature.

### 3.1.3 Orographic enhancement as a function of elevation and barrier height

The precipitation in any elevation band is calculated from the precipitation in the band immediately above or below using the equation (Program equations, see Appendix).

$$P_{I,J,L+1} = P_{I,J,L} * (1+\alpha)$$

where  $P_{I,J,L+1}$  is the precipitation from meteorological station I for day J and elevation band L.

It will be appreciated that the  $(1+\alpha)$  multiplier produces a logarithmic increase in precipitation with elevation. The enhancement factor  $\alpha$  is separately defined above and below a certain elevation which may be specified (ELNORO). Also, when ELNORO is specified, the value of  $\alpha$  will be set to zero when elevation exceeds 1.5 ELNORO.

(Usually a fixed default value of 0.047 is given, which is specified by setting POLKPL equal to 5000 m.)

Below the value of PONORO,  $\alpha_1$  is defined by

$$\alpha_1 = 10^{**} \frac{ELLD}{POLKPL} - 1$$

where ELLD = elevation range per band  
POLKPL = lower precipitation elevation constant

Above PONORO,  $\alpha_2$  is defined by

$$\alpha_2 = 10^{**} \frac{ELLD}{POLKPU} - 1$$

where POLKPU = upper precipitation elevation constant.

#### 3.1.4 Form of precipitation

The model must distinguish between precipitation in the form of snow and precipitation falling as rain and this distinction must be made for each elevation band. Snow is stored until melted whereas rain is immediately processed by the soil moisture model.

The form of precipitation is controlled by three logical statements and the temperature, T, used in these statements is normally the mean daily temperature in each band but it can be specified to be the maximum or the minimum daily temperature in each band.

If  $T < 0^{\circ}\text{C}$  all precipitation is SNOW  
If  $T > \text{AOFORM}$  all precipitation is RAIN.

AOFORM is specified in the parameter deck. If it is not specified or is set below  $0^{\circ}\text{C}$ , it will take a default value of  $2^{\circ}\text{C}$ . Between  $0^{\circ}\text{C}$  and AOFORM a proportion of the precipitation will be specified as rain, and this proportion is defined by FORMPP where.

$$\text{FORMPP} = \frac{T}{\text{AOFORM}}$$

Then rain, RN = PP \* FORMPP  
and snow, SN = PP \* (1 - FORMPP)

#### 3.1.5 Precipitation representation factors

Each meteorological station has two precipitation representation factors associated with it, one for snow, POSREP, and one for rain, PORREP. These factors are introduced because precipitation measured at a point is not always representative of the areal distribution of precipitation. For example, a meteorological station may be in a rain shadow situation, or it may be in a narrow valley where it is receiving precipitation which is more representative of the mountain side some hundreds of meters higher than the station. These representation factors can be determined by comparing long term values of runoff with computed values.

In general, snow measurements are more likely to be distorted by local exposure and orography. As temperatures rise, rain values tend to be more representative because warm rain tends to be more convective nature of the rain makes it more reasonable to introduce an area reduction factor. The program logic is:

If  $TX \leq 0$  use POSREP

If  $0 \leq TX \leq AOFORM$ , use linear interpolation between POSREP and POSREP and PORREP.

### 3.1.6 Evaporation

Evaporation estimation can be subdivided into three processes. In the first process, estimates are made of the daily potential evapotranspiration for the reference meteorological station in the watershed (EVAP). In the second process, this EVAP value is distributed to each elevation mid-band level and is designated by PET. In the third process, PET values are used in conjunction with the calculated soil moisture deficit values to yield an actual evapotranspiration value for each band (AET) and will be discussed in the soil moisture model section.

$$EVAP = AOEDDF * VOEMOF * TX$$

where AOEDDF is an evaporation constant = 0.133

VOEMOF is a factor which is specified as a monthly factor. It accounts for the seasonal variation of EVAP

$$PE(L) = EVAP - 0.90 * APELA$$

Tree cover may also be included in the formulation, as follows:

$$PET(L) = PE(L) * (1.5 * COTREE + 1.0 * (1. - COTREE))$$

where COTREE = fraction of tree-covered area.

The tree covered area can also be modified by a canopy factor, which represents the density of the tree cover. This canopy factor, COCANY, multiplies the tree cover factor, COTREE.

### 3.2 The Soil Moisture Model

The daily amounts of snowmelt and rain are subject to various delays and loss before eventually appearing as river flow at some watershed outflow point. The Watershed Model contains certain logical statements which decide how these snowmelt and rain inputs are subdivided between evaporation loss, and fast, medium, slow and very slow runoff.

The central control parameter for the subdivision of total watershed input is the SOIL MOISTURE DEFICIT. Note that rather than attempting to specify a total soil moisture capacity, the model operates from a lack of soil moisture. When this soil moisture deficit reaches zero, the watershed reaches its maximum runoff potential, except for FLASH runoff which will be discussed later.

A diagrammatic representation of the soil moisture model is shown in Figure 6 and is described below in terms of the priorities of runoff.

#### 3.2.1 First priority: impermeable percentage- fast runoff control

Part of each elevation band can be specified to be impermeable, so that any input of water to this area will enter the fast runoff component. Such runoff can be thought of in terms of surface runoff or very superficial percolation through coarse sediments. Usually such areas must be riparian in nature.

The impermeable percentage of the watershed can be made to vary with soil moisture deficit. The algorithm which describes this process is:

$$\text{Impermeable fraction} = \text{COIMPA} * 10^{**}(-\text{SOSOIL}/\text{POAGEN})$$

COIMPA is the maximum impermeable fraction when the soil is fully



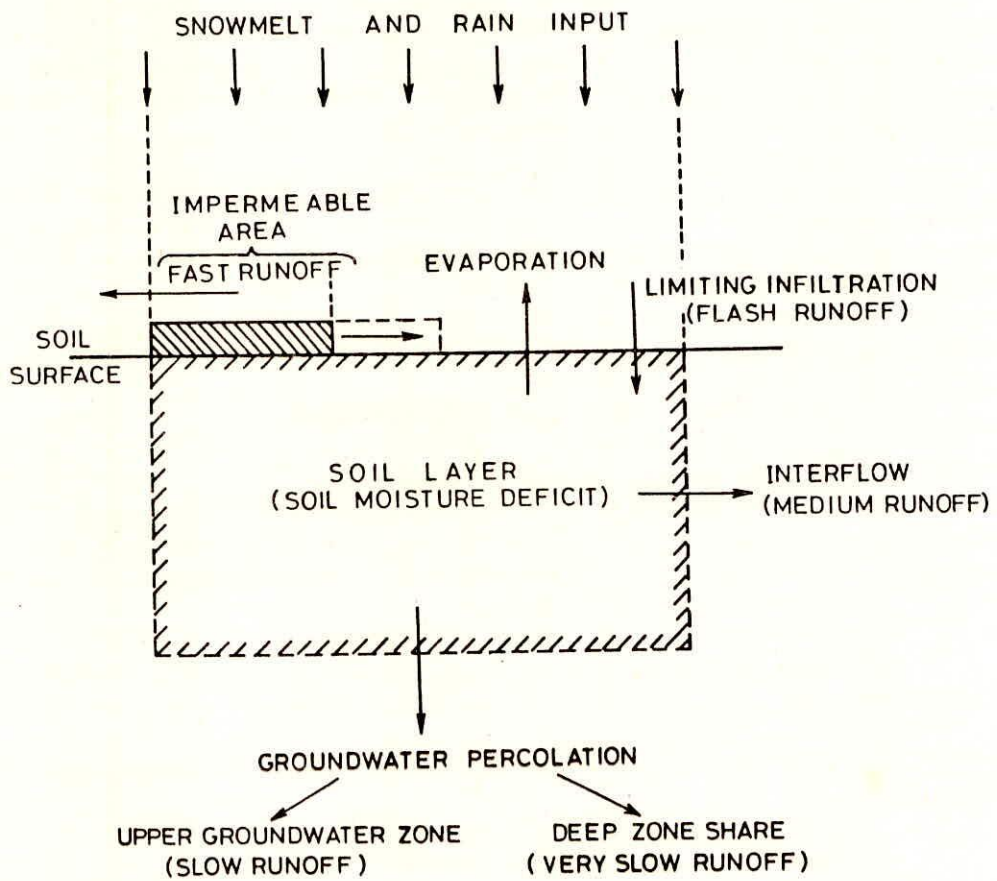


Fig. 6 Model of Soil Layer and Subdivision of Runoff Components.

saturated.

SOSOIL is the soil moisture deficit in an elevation band.

POAGEN is a constant which regulates how sensitive the impermeable area is to changes in soil moisture.

### 3.2.2 Second priority: soil moisture and actual evapotranspiration

Before any further runoff can occur, other than fast runoff, the soil moisture deficit must be satisfied. While soil moisture deficits are being satisfied by incoming water from snowmelt and rain, there is also an evaporative demand which is continually building up a deficit.

Potential evapotranspiration has been described earlier. On any given day, in any given elevation band, there will exist a specified potential evapotranspiration. The soil moisture deficit which exists in that band will represent the actual evapotranspiration capability of that band. The algorithm describing this relationship is:

$$AET = PET * 10 ** (-(-SOSOIL/POEAGEN))$$

AET is the actual evapotranspiration  
PET is the potential evapotranspiration  
SOSOIL is the current value of the band soil moisture deficit  
POEAGEN is a specified constant which controls the rate at which BSD influences PET.

This actual evapotranspiration demand will only influence the area of the watershed which is not impermeable.

For each day a new value of soil moisture deficit is computed:

$$\text{New value of SOSOIL} = \text{SOSOIL} - \text{PRN} - \text{BM} + \text{AET}$$

where PRN is rain input  
BM is snowmelt input

If the band soil moisture deficit reaches zero, any excess water inputs can be subjected to further priorities.

### 3.2.3 Third priority: groundwater percolation

Groundwater percolation accepts any water excess up to a fixed limit (POPERC). Any excess above this limit goes to the fourth priority, medium runoff.

Water which percolates to groundwater is assumed to be divided into specifiable fractions which go to the two groundwater components, the upper groundwater and the deep zero groundwater components. This subdivision of groundwater is controlled by PODZSH, the deep zone share.

Upper groundwater zone recharge =  $(1-PODZSH) * POPERC$

Deep groundwater zone recharge =  $PODZSH * POPERC$

#### **3.2.4 Fourth priority: medium runoff**

Any excess moisture input now remaining is assigned to medium runoff, or interflow. Although this is the lowest priority, it is also frequently the most significant runoff component during active snowmelt and rain storms.

In the model, interflow is considered to be a large reservoir which receives inflows day by day during active snowmelt and rain. These inflows are the excesses remaining after satisfying soil moisture and groundwater abstractions. This reservoir releases a certain fraction each day, but the volume of water released does not immediately appear in the downstream channel system. Instead, this released water undergoes a convolution very similar to the fast component unit hydrograph. This release from an interflow storage reservoir and convolution before reaching the channel outflow point, produces a much more sluggish response for this medium runoff component.

#### **3.3 Watershed Routing**

Water allocated to each of the components of runoff, namely fast, medium, slow and very slow components, are subjected to a routing procedure which produces a time distribution of runoff. The routing procedure for each component is based on the same underlying concept, namely the linear storage reservoir. The fast and medium components of runoff are subjected to a cascade of reservoirs which is essentially identical to unit hydrograph convolution. The slower components of runoff simply use a single linear reservoir, thus avoiding the necessity to convolute for the final outflow.

### 3.3.1 Fast runoff routing

The watershed model calculates unit hydrograph ordinates for convolution of fast runoff. The calculation is based on a conceptual model of the runoff process developed by Nash in which inflows are passed through a cascade of linear reservoirs. The resulting outflow at time  $t$  from a unit impulse of inflow is:

$$u(t) = \frac{1}{k^n} \cdot \frac{t^{n-1}}{(n-1)!} \cdot e^{-t/k}$$

$K$  is the linear storage constant for each of the reservoirs in the cascade.

$n$  is the number of linear reservoirs in the cascade (specified by NRESVO).

$t$  is the time after the water input has occurred.

The watershed model uses the above equation to calculate unit hydrograph ordinates for each day.

Linear reservoir routing of the components of runoff is computed as follows:

$$\text{First reservoir : } Q_1 = Q_1 + (1/(1+TK)) + (WB - Q_1)$$

$$\text{mth reservoir : } Q_m = Q_m + (1/(1+TK)) * (Q_{m-1} - Q_m)$$

where  $Q_m$  = outflow from the mth linear reservoir  
 $TK$  = time constant of the linear reservoir (This can be POFSTK, etc.)  
 $WB$  = water input to the first linear reservoir.

### 3.3.2 Medium runoff routing

The medium speed runoff, often thought of as an interflow component, undergoes a two stage routing process. In the first stage the medium runoff for each day enters a linear storage reservoir with a release constant INTK. The daily release from this reservoir is therefore a constant percentage of the total storage on any given day. Such a release represents an exponential decay which is identical to Nash's result with the

number of reservoirs equal to one.

$$QI = QI + (1/(1+INTK)) * (WI - QI)$$

where WI is the water input to the interflow reservoir, and INTK can be either POIS<sup>T</sup>TK for snow runoff or POIRTK for rain.

The daily release QI is then subjected to time distribution by convolution with a unit hydrograph which is similar to the fast unit hydrograph.

### 3.3.3 Slow runoff routing

The slow components of runoff, usually termed groundwater flow or base flow components, are divided by the soil moisture model logic into a slow, upper-zone component and a very slow, deep-zone component.

Both of these groundwater components are routed using a single linear reservoir which accumulates each days inflow and releases a fixed percentage of the total storage each day.

## 3.4 Snowmelt Budget

The watershed model accumulates precipitation falling as snow and then depletes these snowpacks according to the calculated melt rate. This snow accumulation and depletion is carried out separately in each area-elevation band. There are two ways in which this snow budgeting can be carried out. The first being a simple budget at the mid-band, elevation, referred to as a block budget, and the second being a more complex wedge computation. It is one of the model options to select either the simple block budget or the wedge budget.

### 3.4.1 Block budget

From a computational viewpoint this is a straight forward calculation procedure in which snow is accumulated as if it was falling at the mid-elevation of each band. Snowmelt calculations are also made at this mid-band elevation.

### 3.4.2 Wedge budget

This analysis option recognizes that the final depletion of snow is a gradual recession of snowline from the bottom to the top of a band. In this option there is a smoother transition as snow is depleted completely from a band. It might be commented that the advantages of this more complex analysis are not as great as might be thought. However, if snow gradients are high, as can be the situation under some melt conditions, then the wedge budget does give a better representation of runoff behaviour.

Essentially the wedge budget still uses the block budget methods until the elevation band below is out of snow. At this point in time the wedge analysis taken over.

A set of calculations is still carried out at the mid-band elevation. When the snowpack is depleted to a value defined by SOPATS (usually of the order of 400 mm of water equivalent) a partial area of snowcover is computed as further melt occurs.

### 3.5 Snowmelt and Simplified Energy Components

The UBC watershed model contains two options for the calculation of snowmelt:

1. An energy budget approach which is simplified for use when there is only temperature data available. (The method is also easily usable if more detailed radiation, albedo and wind data are available).

The choice of snowmelt method is governed by the parameter ROERGY.

If ROERGY = 0, the energy method is used.

If ROERGY = 1 (or any non-zero value), then the degree-day method is used.

2. A degree-day approach in which two equations are used, one for forest melt and one for open area melt.

From the consideration of various energy exchange processes represented in the next section, it is clear that, in dense forests, the longwave heat exchange processes dominate and consequently a temperature index approach is reasonably valid. However, in open areas, an energy approach is superior because

shortwave radiation and snowpack albedo are very important. Also the convective and condensation melt components are increased by turbulent mixing induced by wind and rugged topography. Temperature alone is not an adequate indication of melt because temperature varies with elevation and with incoming airmass, so that there is a weak and non-linear relationship between temperature and shortwave radiation. Albedo varies seasonally, but can rise considerably during periods of new snowfall, so that net solar radiation is a non-linear function of albedo. Cloud cover can greatly reduce the shortwave radiation and also has a strong influence on the longwave radiation balance. This raises the question of how well cloud cover can be estimated, especially its density, and to what extent the reduction in shortwave radiation is compensated by the increased in net longwave exchange. The conclusion from our extensive studies appear to be that open area melt is not a simple linear function of temperature, but relationships are put forward by which temperature may be used to estimate the various non-linear inputs which control the following simplified energy method for the calculation of snowmelt.

The energy exchange at the surface of a snowpack is made up of four major components:

1. The shortwave radiation exchange, consisting of incoming solar radiation, and the reflected outgoing shortwave radiation. This shortwave component depends on the time or of year, the site exposure, cloud cover, and snow albedo.
2. The longwave radiation exchange depends on black body radiation from the snow itself and from clouds and tree cover, and gray body radiation from the overlying airmass. Under clear skies, the net longwave is outgoing, or negative, unless air temperature exceeds about 20°C. Under cloudy conditions and also under tree cover net longwave can be positive at temperatures above freezing.
3. Convective heat transfer is produced by turbulent heat exchange between the airmass immediately above the pack. This heat transfer is dependent on both wind and air temperature and particularly on the stability of the airmass above the snowpack. A warm airmass above the cold snow surface tends to be stable, resisting any downward transport of heat to the snowpack, unless there is enough wind to produce turbulent mixing. This

turbulent heat transfer is governed by the Richardson number,  $R_I$ , which is a measure of stability. The bulk

Richardson number, defined below, is essentially the air temperature divided by the wind speed squared. As air temperature increases, and if the wind is only moderate, the stability can increase to the point where very little convective heat transfer can occur. Convective heat transfer is therefore self limiting and becomes quite small at higher air temperatures, unless there is very strong wind.

4. Advective heat transfer, often termed condensation melt, is caused by the transport of moisture to and from the snowpack. Whether condensation occurs, releasing latent heat to the snow, or whether evaporation occurs, cooling the pack, depends on the relative vapour pressures of the air and the snow surface. Wind is once again an important factor and so is stability, as was discussed for convective transport. Advective heat transport can therefore produce snowmelt if the dewpoint temperature is above freezing, but, like the convective heat transport, becomes limited at higher temperatures by the stability of the warm airmass.

A simple set of equations has been developed which expresses the various snowmelt components in terms of millimeters of snowmelt per day, either negative or positive. Various simplifying assumptions have been used to write these equations, but they have been tested on high quality data sets from the U.S. Corps studies (1954) and are a considerable improvement on the calculation of snowmelt and glacier melt, especially for high elevation, open area regions in the mountains. The Simplified energy components are given below:

#### 3.5.1 Net shortwave - energy input

$$\text{Melt} = I_S (1 - C_L) (1 - A_L) \text{ mm/day}$$

where  $C_L$  is closed cover,  $A_L$  is the albedo of the snowpack and  $I$  is the incident solar radiation, which varies seasonally and with latitude and with atmospheric conditions. At  $35^\circ$  North,  $I_S$  can be expressed in terms of millimeters of melt equivalent per day instead of Langley per day,



$$I_S = 54 - 29 \cos 2\pi N/365 \text{ mm/day}$$

The albedo and cloud cover reduce the potential melt values of equation to the net values expressed by above equation.

### 3.5.2 Longwave Radiation

Stefan's law can be expanded in terms of the temperature above freezing,  $T$ , so that the longwave black body radiant energy,  $I_L$ , can be expressed as a linear function of temperature plus small higher order terms,

$$\begin{aligned} I_L &= \sigma (273 + T)^4 \text{ Langleys/day} \\ &= \sigma 273^4 (1 + 4T/273 + 6T^2/273^2 + \dots) \\ &= 661 (1 + 0.015T + 0.0001T^2 + \dots) \text{ Langleys/day} \\ &= 82.6 (1 + 0.015T + \dots) \text{ mm/day} \end{aligned}$$

Under clear sky conditions in an open, tree free, area, the net longwave radiation received by the melting snowpack is the difference between the black body radiation of the  $0^\circ\text{C}$  snowpack and the incoming gray body radiation from the clear sky. Various estimated values for the grey body radiation are available, some of which are quoted in the U.S. Corps snowmelt report (1955). All of the equations show a small dependence on humidity of the atmosphere, such as equations due to Brunt and Angstrom. The simplest equation, from the Lake Hefner study is,

$$I_{LA} = \sigma T^4 (0.749 + 0.0049 e_a)$$

where  $I_{LA}$  is the atmospheric longwave radiation, and  $e_a$  is the vapour pressure in millibars. The dependence on vapour pressure is so small that it is reasonable to accept the value.

$$I_{LA} = 0.757 \sigma T^4$$

The net clear sky incoming longwave radiation,  $I_{LN}$ , can therefore be written as:

$$I_{LN} = 661 (0.757 (1+0.015T_A) - (1+0.015T_S)) \text{ Langleys/day}$$

where  $T_A$  is mean air temperature and  $T_S$  is the snow surface temperature, which is zero for a melting snowpack.

$$I_{LN} = 7.51 T_A - 161 - 9.92 T_S \text{ Langleys/day}$$

In snowmelt equivalent,

$$I_{LN} = 0.94 T_A - 20.1 - 1.24 T_S \text{ mm/day}$$

For a melting snowpack,  $T_S$  is zero, and  $I_{LN}$  does not become positive until  $T_A$  exceeds 21.4°C.

### 3.5.3 Net longwave under cloudy conditions

Clouds temperature,  $T_C$ , act as black bodies, so that under 100% cloud cover, the net incoming longwave,  $I_{LNC}$ , is,

$$\begin{aligned} I_{LNC} &= 9.92 (T_C - T_S) \text{ Langleys/day} \\ &= 1.24 (T_C - T_S) \text{ mm/day} \end{aligned}$$

The clear and cloudy sky equations are combined into an expression for the net longwave exchange,  $I_{LNT}$ , for a partial cloud cover fraction,  $C$ , so that, for a melting snowpack at 0°C,

$$I_{LNT} = (-20 + 0.94 T_A) (1 - C) + 1.24 T_C \cdot C \text{ mm/day}$$

The cloud temperature can often be approximated by the dew point temperature, which is approximately the minimum air

temperature.

#### 3.5.4 Convective and advective heat transfer

The U.S. Corps report (1955) and Anderson (1976) present equations for convective and advective heat transfer. Anderson refers to the question of air mass stability, but does not incorporate the results into a final relationship. The following equations are an approximate estimation of the net heat transfers which have been developed from the earlier work.

Under neutrally stable conditions the convective heat transfer,  $Q_C$ , is approximately,

$$Q_C = 0.113 (p/101) T_A \cdot V \text{ mm/day}$$

in which  $P$  is the atmospheric pressure in  $\text{kN/m}^2$  for the elevation being considered,  $T_A$  is the mean temperature and  $V$  is the wind speed in kilometers per hour.

Similarly, the advective, or condensation, melt  $Q_A$  under neutrally stable conditions is approximately,

$$Q_C = 0.44 T_d \cdot V \text{ mm/day}$$

where  $T_d$  is the dew point temperature, which can be approximated by the minimum air temperature.

#### 3.5.5 Rainmelt

Snowmelt from rain BMR is computed as follows:

$$\text{BMR} = K * T_M * \text{RN}$$

where  $K$  = a constant, and  $\text{RN}$  = rainfall.

This formula assumes that the rain falls at the mean air temperature and the  $K$  factor ( $\text{mm}/^\circ\text{C}$  of rain) represents the heat content of the rain. This equation is also used in the energy method.

#### 3.6 Application of the Simplified Energy Snowmelt Equations

There are advantages to be gained from using energy equations for calculating snowmelt. The physical basis of the equation makes it possible to estimate snowmelt for forested and open conditions, for clear or cloudy weather, for various slope and aspects of mountainous watersheds and for changes in elevation. It is also possible to argue the impacts of changing forest cover or the snowmelt that would be experienced under extreme and unusual weather sequences. Some simplified energy relationships will be tested against measured point snowmelt data for both open area melt and forested area melt.

For most high mountain regions data on radiation, cloud cover, etc., are not available. The factors which must be described are the cloud cover, albedo, wind, cloud temperature and dew point temperature. All other factors can be estimated from known physical behaviour. As reasonable approximations, it has been found possible to represent these various factors with temperature-based estimates.

### 3.6.1 Cloud cover

The cloud cover has been assumed to be related to the daily temperature range.

$$(1 - C_L) = (T_{MAX} - T_{MIN}) / D_R$$

in which  $C_L$  is the cloud cover fraction,  $T_{MAX}$ ,  $T_{MIN}$  are the daily maximum and minimum temperatures, and  $D_R$  is the daily temperature range for open sky conditions at a certain elevation in the watershed.

### 3.6.2 Wind estimate

The wind tends to produce a decrease in daily temperature range, so that cloudy conditions are also windy conditions.

$$V_b = K_R = (T_{MAX} - T_{MIN})^{-1/2} - K_V$$

in which  $K_R$  and  $K_V$  vary slightly with elevation.

### 3.6.3 Albedo

The albedo is modelled by three relationships. Fresh snow is assumed to settle and change its albedo from a starting value of 0.9, which then decays by a factor of 0.9 per day until it reaches a settled value,  $A_{LS}$ , of 0.7, as described by the following equation:

$$A_{LS(j+1)} = 0.9 A_{LS(j)} \quad 3.6.3.1$$

in which  $A_{LS(0)}$  starts at 0.9 and  $A_{LS(j+1)}$  is greater than or equal to  $A_{LS}$ , usually 0.7. Then the albedo continues to decrease at an exponential decay rate, which is controlled by the calculated cumulative melt for the season given by

$$A_{Lj} = A_{LS} e^{-\Sigma M/K_L} \quad 3.6.3.2$$

where  $A_{LS}$  is the settled value, usually 0.7,  $\Sigma M$  is the cumulative seasonal melt in millimeters and  $K_L$  is a constant, approximately of the order of the total seasonal melt, usually taken as 4000 mm.

When new snow occurs, if it is greater than 25 mm, the albedo is assumed to return to a value of 0.9. The albedo then decays again at the 0.9 rate, specified by equation (3.6.3.1), but continues down until it reaches the value computed on the day before the snow occurred,  $A_{Lj}$  from equation (3.6.3.2). The underlying recession described by equation (3.6.3.2) then takes over. This process allows a fairly rapid change of albedo from 0.9 to 0.7, or down to the calculated  $A_{Lj}$  value from equation (3.6.3.2), and then a slow recession as the season advances to albedo values of 0.4 or even 0.3 for very deep and aged snowpacks. Snow cover on a glacier is treated in the same manner, but the glacier, when it becomes free of snow, is assumed to have an albedo of 0.3.

These relationships for cloud cover, wind and albedo have been developed using SIHP (1986, 87, 88) data gathered in the Himalayas and also using U.S. Corps of Engineers data gathered in great detail for the Central Sierra Snow Studies (1952) as discussed by Quick (1987).

The following information is required for the operation

of model-

1. the temperature range which controls cloud cover specified by the parameters AFOGY, AOSUNY, AFOGX, where AFOGX is the maximum range for a station AFOGY is the range below which complete cloud cover exists, and AOSUNY is the range above which the sky is assumed clear.

This temperature range depends on the elevation of the meteorological station and decreases as elevation increases. Typical values are specified in the calibration parameter files for the various watersheds.

2. the percentage of forested and open area.

3. the aspect: the area and slope of north and south facing region of the watershed and the topographic barrier height at sunrise and sunset.

### **3.7 Alternative Snowmelt Routine: UBC Degree-Day Method**

A simple melt formulation, based entirely on air temperatures has been set up in the following manner. Convective heat transfer is represented by the mean daily temperature above freezing. This term requires no further adjustment: if the mean temperature is equal to or less than freezing, then no convective melt will occur. The net radiant energy is considered to be well represented by the daily temperature range, namely the maximum daily temperature minus the minimum daily temperature. But this term will only produce melt if the minimum temperature is above freezing. The underlying assumption here is that the minimum temperature is a good estimate of the dew point and so represents the vapour pressure relative to that of the snow surface. The minimum temperature is used as a linear switch, or multiplier, and controls how much of the radiant energy contributes to snowmelt and how much produces sublimation.

The third important energy source or sink is condensation to, or evaporation from the snowpack. This term is controlled by vapour pressure of the air compared with the vapour pressure of the snow surface. Again the minimum temperature is used and an estimate of dew point. The rate of condensation is determined by multiplying the dew point above 0°C by the linear multiplier based on minimum temperature.

The resulting snowmelt formulation is specified in two different forms, the first for forested areas of the catchment and

the second for open areas.

### 3.7.1 Forested melt formulation

$$\text{Band Melt BM} = (A + \text{HM2MOF} * (\frac{\text{TD}}{\text{PODIUF}} + \text{TN})) * \text{AOMDDF}$$

BM	=	Band melt for a particular band mid-elevation
AOMDDF	=	Point melt factor
A	=	Mean daily temperature of the band
HM2MOF	=	Energy partition multiplier, defined below
TD	=	Daily temperature range (TX-TN) in the band
TX	=	Band maximum daily temperature
TN	=	Band minimum daily temperature
PODIUF	=	Radiant energy factor
HM2MOF	=	$\frac{\text{TN} + \text{TD}/\text{PODIUF}}{\text{PODEWP} + \text{TD}/\text{PODIUF}} < \text{AOMODX}$

Note the restriction on the maximum value of HM2MOF

PODIWF = Reference dewpoint controlling energy partition between melt and sublimation.

Note that the TD/PODIUF portion of the multiplier permits some radiation melt on days when TN is a little below freezing but the maximum temperature goes somewhat above freezing.

### 3.7.2 Open-area melt formulation

This melt formulation can be specified above the tree-line and in open areas.

$$\text{Band Melt BMO} = \text{AOMDDF} * (\text{TX} + \text{HM2MOO} (\text{TN})) * \text{MMF} \quad (3.7.2)$$

where MMF is specified as a monthly factor.

In these open areas, the radiation component of melt is far more significant, so that melt is more dependent on the maximum daily temperature than on the mean.

A similar open area melt formulation is used for the depletion of glaciers, where BMG is the glacial band melt.

$$BMG = KG * MBO$$

(3.7.2.2)

where KG is a constant  $\geq 1.0$ .

This formula assumes that the rain falls at the mean air temperature and the KG factor (mm/°C of rain) represents the heat content of the rain. This equation is also used in the energy method.

### 3.7.3 Negative melt budget

If temperatures have been below freezing for any length of time, the snow becomes deeply frozen and requires ripening before melt can occur. These antecedent conditions are accounted for by keeping a running sum of antecedent mean temperatures, and allowing the total to decay by a certain fraction each day, specified by CCTK, the antecedent negative melt time constant. This decaying of the negative melt budget is essentially a "forgetting" process, so that the negative melt budget depends primarily on temperatures that have occurred over about the previous 10 days or so. The memory of earlier cold temperature decays away. The ripening of the snowpack takes into account thermal input from rainfall, and further accounts for time delays induced by the water holding capacity of the snowpack. The ripening of the snowpack is computed as follows:

$$CC = CC + (1/(1+CCTK)) * (CCB - CC) \quad (3.7.3)$$

where

CCB	=	TM + KCC*RN
CC	=	cold content storage, and KCC is a constant.
KCC	=	latent heat contribution from freezing of rain falling on snowpack

A percentage of meltwater can be retained by the snowpack and this water holding capacity of the snowpack is expressed as a simple fraction of the cumulative snowfall.

### 3.8 Runoff from High Intensity Rain

There are two different controlling mechanisms for runoff from a watershed system. The runoff from moderate intensity rain and snowmelt events can be considered to be controlled by soil moisture levels and this is the normal operation of the UBC Watershed Model. The runoff from high intensity events is



controlled by the rate at which water can infiltrate into the soil system and these infiltration rates are relatively independent of soil moisture levels.

For these high intensity rain events, some of the precipitation infiltrates into the soil system and is subjected to the normal soil moisture budgeting. The fraction of the rain which does not infiltrate is considered to contribute directly to the fast runoff component and is referred to as the FLASH SHARE.

It should be noted that even intense snowmelt rates do not appear to be adequate to produce FLASH runoff, even though 75 mm of snow may melt in the day. Apparently, this snowmelt is released to the soil system steadily over the whole day and the rate of release is below the infiltration capacity. In contrast, rain events of even less than 50 mm in the day can exhibit flash behaviour. Examination of rain intensity data suggests that rainfall events of this magnitude tend to occur in localized periods, or bursts, of high intensity rain, intensities which can be higher than the soil infiltration rates. The relationships governing FLASH SHARE behaviour are as follows:

1. The portion of the total daily precipitation which is subjected to the normal soil moisture budget system is

$$(1-MFR) * (1-PMXIMP) * PRN \quad (3.8.1)$$

where

MFR	=	(MR-VOFLAS)/VOFLAX
MFR	=	FLASH SHARE fraction (MFR ≤ 1.0)
PMXIMP	=	IMPERMEABLE percentage of the particular watershed elevation band
NR	=	total daily precipitation
VOFLAS	=	threshold value of total precipitation for flash runoff
VOFLAX	=	maximum value of total precipitation, which limits MFR range.

2. The portion of the total daily precipitation which flashes off is therefore, by difference,

$$(MFR) * (1-PMXIMP) * PRN \quad (3.8.2)$$

3. From the fraction of the watershed which is calibrated to be impermeable, the total daily precipitation input is assumed to go to fast runoff, and this would be true with or without the FLASH SHARE mechanism.

4. When high intensity rain occurs at the same time as snowmelt, the snowmelt is added to the rain and subjected to FLASH SHARE.

5. The FLASH SHARE mechanism only operates when it is specified. In theory, with adequate precipitation data, the FLASH mechanism could be made automatic. In practice, some point rainfalls, although intense, are so localized that there is limited watershed response of any kind. It has therefore proved more satisfactory to identify FLASH events by careful inspection of the river flow and meteorological data.

6. It should be noted that FLASH is specified by only one parameter, FLASHR. The actual flash response is coupled to the normal watershed calibration by incorporating PMXIMP, the percentage of the watershed which behaves as if it was impermeable. With the usual gradient of impermeability which is observed to exist in mountainous watersheds, the run-off from lower elevations in more regulated areas, whereas the higher elevation, where PMXIMP is higher, automatically behave as much faster run-off regions.

7. Rain inputs for FLASH can be specified in two ways. Rain can be specified as the observed rain at a station and can be increased by the elevation parameter for rain. Alternatively, the rain can be specified for each elevation band.

An important aspect of any watershed model is the stability of the calibration from year to year, for example, it is important to test whether flood and drought sequences can be correctly calculated with the same set of hydrological parameters. Errors may arise from two primary sources. Firstly, there may be errors in the meteorological data inputs, especially rainfall, and such errors can only be inferred from the streamflow response. Secondly, errors may result from incorrect description of watershed behaviour which includes incorrect allocations to the fast and slow runoff components. Because the calibration of a watershed model depends on the accuracy of meteorological inputs and streamflow outputs it is feasible to identify really large and obvious errors in either streamflow or precipitation values.

A common problem with the rainfall is the correct evaluation of point rainfall in terms of areal distribution. Such problems are handled by adjusting representativeness parameters for the precipitation. Precipitation gradient is considered a function of elevation and adjusted by comparing observed and computed streamflows. The areal distribution of precipitation is the most important aspect of calibration and has the biggest influence on model performance because snowpacks are accumulated by the model from the measured precipitation and from precipitation-elevation relationships. If snow course data are available at even few locations in the watershed, it helps in evaluation of precipitation representativeness and gradient parameters by checking calculated snowpacks against recorded snow courses after the winter season.

As described earlier, the runoff calculation parameters subdivide rain and snowmelt inputs into fast, medium and slower components of runoff. Options exist to specify various parameters such as the impermeability parameters, the evapotranspiration control parameter in each band and the parameter controlling the allocation to the upper and lower groundwater zones. The times at which these components of runoff appear in the stream system are evaluated by systematic examination of different portions of observed hydrograph response. The graphical output is especially useful for evaluating shape reconstitution.

To test the stability of watershed calibration parameters, the calibration of the model is carried out by operating continuously for a number of years of data at a time. This continuity in data results in higher accuracy because the long term moisture status can be checked. The start of model

operation is preferred to be just before the winter season so that snowpack may be built up by the model using the data of a complete season.

In this study, the UBC Watershed Model is being calibrated for forecasting flows on the upper Satluj River system. This study has identified certain key issues which are central to achieving satisfactory forecasting results, and these issues are set out below.

#### 1. Precipitation distribution

All watershed modelling depends on achieving an accurate estimate of precipitation distribution across the basin. In mountain regions there is a strong orographic pattern of precipitation which tends to be reasonably repeatable from year to year. Generally, precipitation increases at a certain rate with elevation and this rate can be estimated if there are sufficient data stations at various elevations in the basin. This data may be from standard meteorological stations with daily measurements of precipitation and temperature, or from snowcourse or snowpack measurements. If data is only available at one or two locations, then precipitation gradients may have to be assumed and then modified by comparing computed and measured runoff from the watershed. For this study such results are shown in Figure 7.

This iterative approach for determining precipitation gradients is only possible when dealing with snowmelt because snowmelt can be calculated from temperature which is also a function of elevation. Therefore, there are two definable constraints, firstly, the volume of runoff in the melt period and secondly, the snowmelt potential as a function of elevation. A third constraint is needed to be able to solve for the actual precipitation gradient, this third condition is the assumed form of the precipitation gradient. For example, if the gradient is assumed to be linear, or logarithmic, or some other functional form, then a unique solution can be found. Such a solution cannot be found for rainfall, and therefore it may be necessary to assume a similar gradient as for snow, or else much more data must be collected at different elevations to determine the gradient.

There are special problems with the orographic precipitation pattern in the northerly Himalayan watersheds, and these problems appear to be common for the whole region. The main feature of the precipitation is that the weather systems have to enter the region by crossing over high mountain barriers. On the upslope side of these barriers, there is a strong increase of

Figure 7 : Variation in mean seasonal winter precipitation with elevation

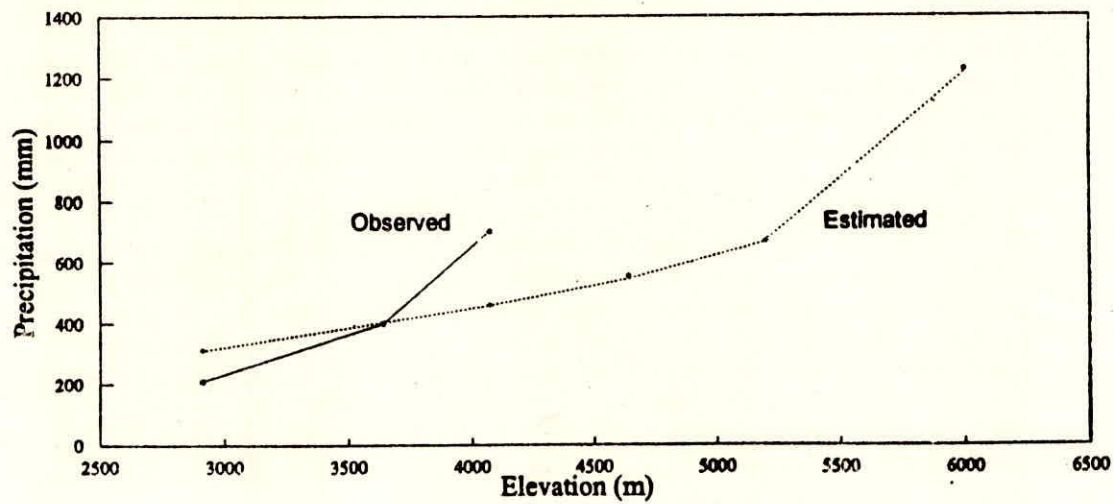
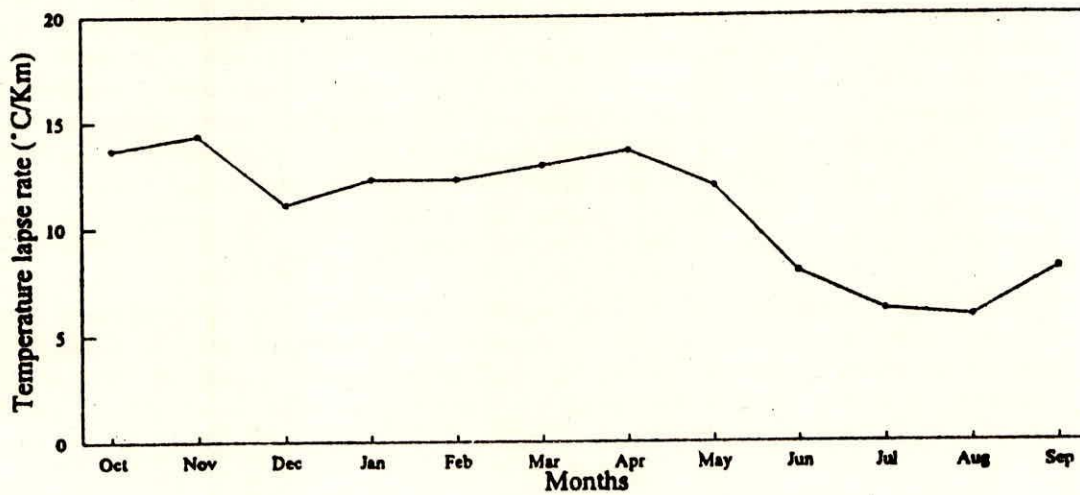


Figure 8 : Mean monthly temperature lapse rates between Namgia and Kaza



precipitation with elevation and much precipitation falls. However, on the lee side of the mountain barriers, which is the region under study, there is high precipitation at the high elevations, but, as the weather systems move in the downslope direction, there is a rapid decrease in precipitation. This decrease is typical of so-called subsidence zones and consequently valley precipitation can be quite small, and is frequently zero. This pattern of precipitation is a major difficulty for making accurate forecasts, because most data stations are located at mid to lower elevations where precipitation is relatively low. Clearly, it is difficult to use these low values or even zero values of precipitation to estimate the much higher precipitation occurring at upper levels.

It should be noted that in another region of the Himalayas, precipitation data was available for the weather side of the mountain barrier where the precipitation was much greater. This data proved to be a very good indicator of precipitation for the mountain peak region and the lee side, subsidence zone. That particular study (Quick and Pipes, 1989) clearly illustrates the importance of using these high, upwind side precipitation measurements. In that particular study, the subsidence effect was so strong that valley precipitation in the northerly mountain region was essentially zero, so that estimating high elevation precipitation from the valley data was clearly impossible.

## **2. Temperature distribution**

To estimate snowmelt, it is necessary to estimate temperatures as a function of elevation in the watershed. Examination of measured temperatures at two elevations in the Spiti catchment indicates that lapse rates are quite variable, but fortunately somewhat systematic (Figure 8). In the winter, cold weather period quite high lapse rates of  $-10$  to  $-14$ °C per km are observed. Such a high lapse rate is surprising, because anything in excess of  $-10$ °C per km, the dry diabatic lapse, is unstable and should induce mixing. However these stations are separated horizontally by quite a number of kilometers, and perhaps the airmass temperature is modified by the time it reaches the valley region. Fortunately, the lapse rate during the melt season is much closer to the usual value of  $6.4$ °C per km, which is the pseudo or saturated adiabatic lapse rate.

As mentioned earlier, UBC watershed model has two methods for calculating temperatures as a function of elevation. One method computes temperatures using a variable lapse rate which is a function of the daily temperature range. Briefly, if there is a

small daily range, the weather is probably cloudy and temperatures will decrease at the saturated adiabatic rate of  $6.4^{\circ}\text{C}/\text{km}$ . Alternatively, if the daily temperature range is large, then the weather is probably clear sky and temperatures will decrease at the dry adiabatic rate of  $10^{\circ}\text{C}/\text{km}$ . The second method computes lapse rate using daily temperatures at a high and low station in the watershed. This method is very useful if the temperature stations are not too far apart horizontally, but in the present study the first method has proved better.

### 3. Melt seasons

Two distinct melt season periods need to be recognized, although they will be seen to overlap and interact to some extent. From April to June there is a snowmelt season which may extend to late June or even into July for heavy snow years. From June to September the glaciers become snow-free and glacial melt season contributes to runoff. These two seasons interact because in a heavy snow year, the glaciers will remain snow-covered for a longer time which will reduce glacial melt. Because the snow has a higher albedo, the snowmelt runoff will be less than the runoff that would occur from a snowfree glacier. In contrast, for a low snow year, the glaciers will be free of snow earlier, and although snowmelt will be less, there will be a greater contribution from the lower albedo glaciated regions. If the glaciated areas are significant, increased glacial runoff can therefore compensate to some extent for low snowpacks during a low precipitation year. The watershed model estimates snowpacks and computes when the glacial areas are snowfree. The model also computes albedo of the snowpack as the season progresses and these values are used in snowmelt routine.

## 5.0 APPLICATION OF UBC WATERSHED MODEL TO SATLUJ RIVER

The streamflow simulation of Satluj river at Rampur has been carried out using three years of meteorological data for which stream flow data exists. Fortunately, the watershed considered for this study has meteorological stations located at different elevations and have daily data for the whole year. The flow data is available at two sites, namely, Namgia and Rampur. A separate gauging site is maintained for the Spiti basin near Namgia. The advantage of this gauging site will be discussed later.

The study was initiated by considering the whole watershed as a single unit having elevation range from 1500 m to 7026 m. Two meteorological stations, namely, Kalpa (2439 m) and Kaza (3639 m) were assumed to represent the lower and upper part of the basin respectively. The representativeness and precipitation gradient parameters were estimated comparing the simulated and observed streamflows. The temperature lapse rates computed by the model using daily temperature range data were used throughout the calculations. The air temperature of 2°C was considered to distinguish between rain and snow during precipitation. The model was allowed to operate automatically for the continuous 3 years of data so that all model parameters controlling snowmelt and runoff were held constant and snowpacks were accumulated and depleted each day by the model. The soil moisture conditions were generated automatically by the model. The simulation was started from the month of October when the major part of the flow is from the groundwater component. The simulated and observed flows are illustrated in Figures 9(a) & (c).

Because the Spiti flows are separately gauged, it was possible to split the total watershed into two sub-basins, namely, an upper sub-basin (Spiti) and a lower sub-basin covering about 10070 and 6475 sq.km. area respectively the lower sub-basin covered the whole area of study watershed other than Spiti. Various combinations of meteorological stations were tested for these sub-basins and the best results were obtained using Namgia and Kaza for the upper basin, and Kalpa and Namgia for the lower sub-basin. The total basin outflow was calculated by simply adding the flows, because the channel routing time was estimated to be in the range of 8 to 10 hours. The results for the upper and lower sub-basins are presented in Figures 10(a) to (c) and Figures 11(a) to (c), respectively. The total basin simulation as the combination of two sub-basins is shown in Figures 12(a) and (c).



Figure 9(a) Observed and simulated streamflows for the year 1987/88 considering watershed as a single unit

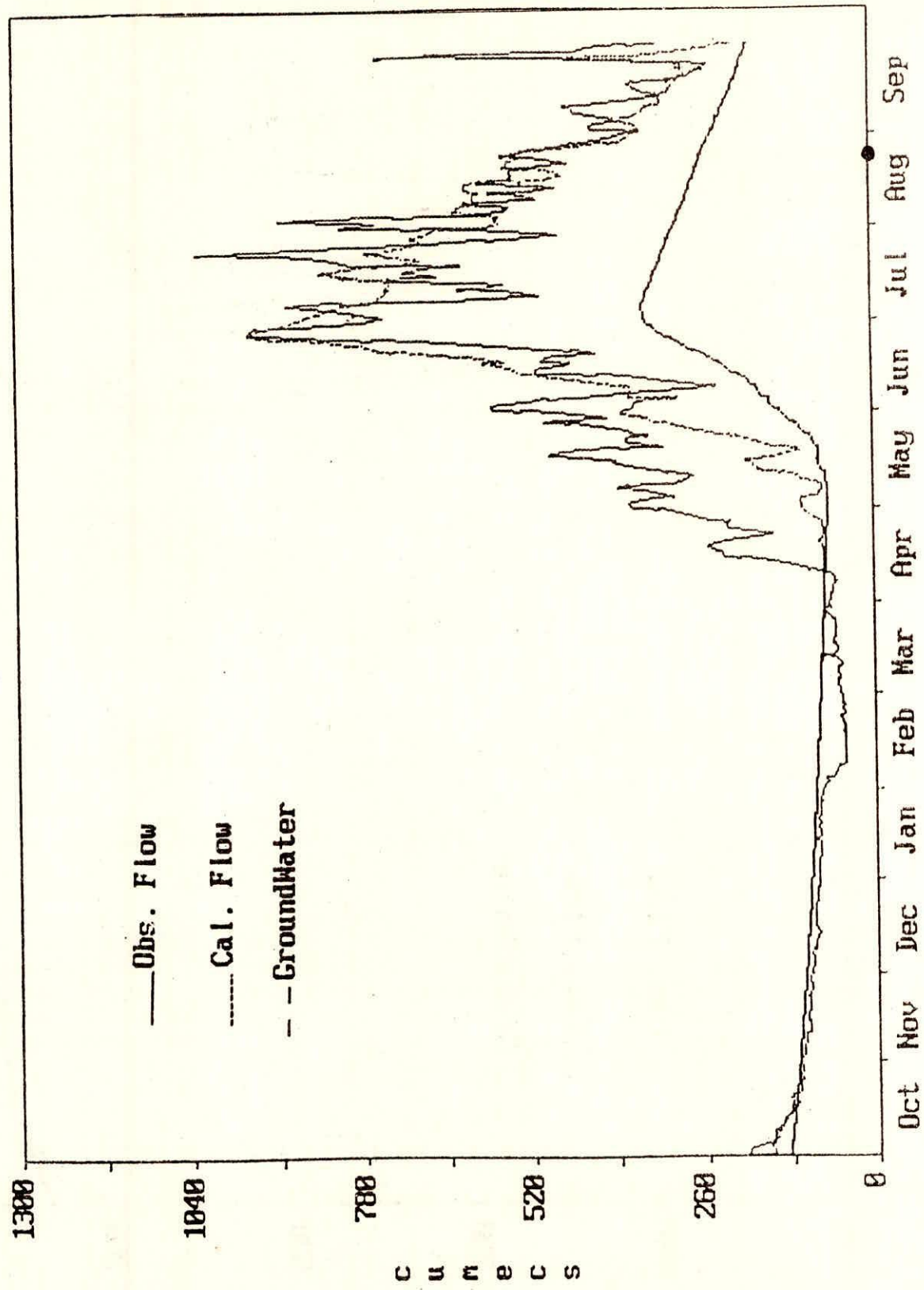


Figure 9(b) Observed and simulated streamflows for the year 1988/89 considering watershed as a single unit

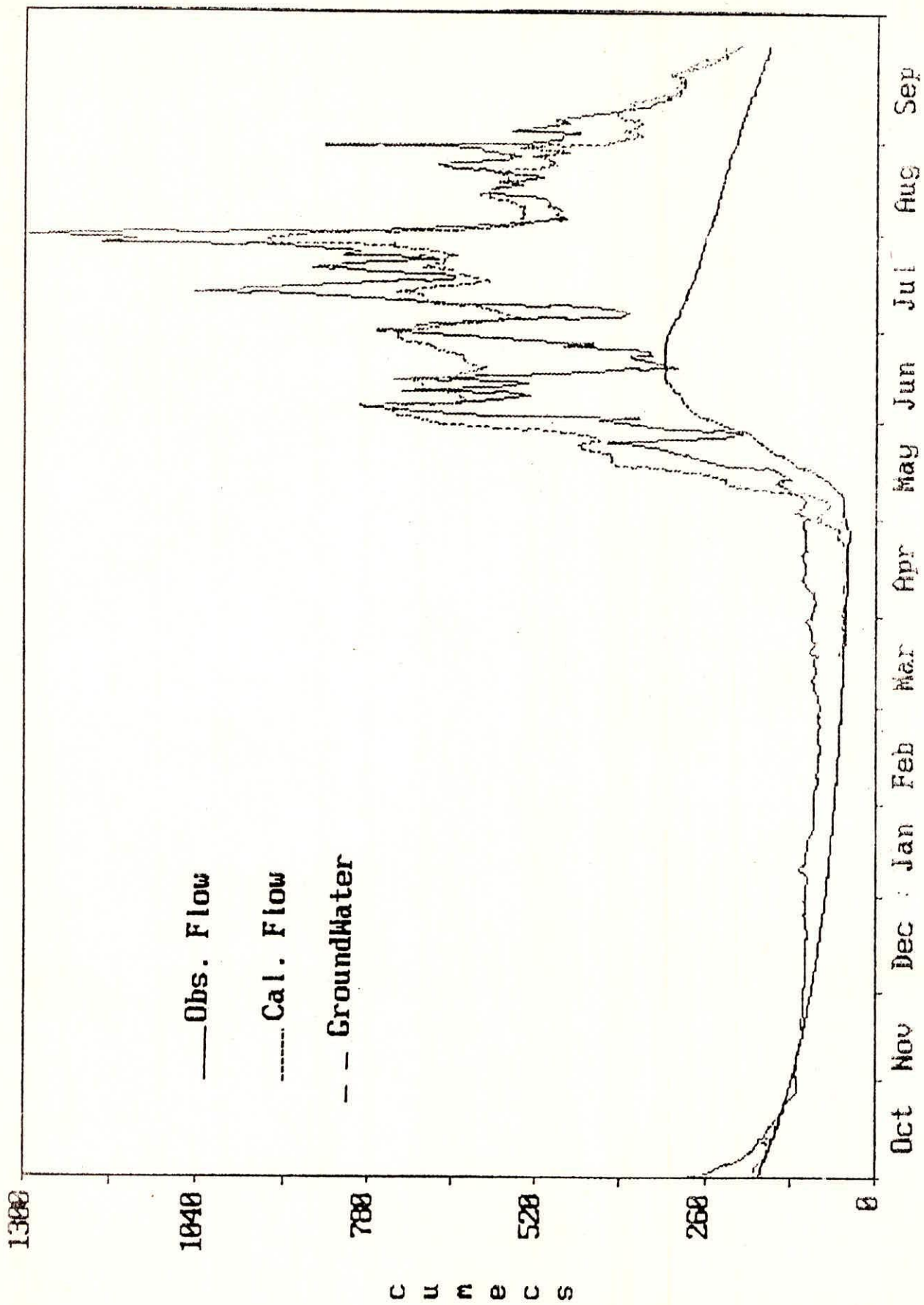
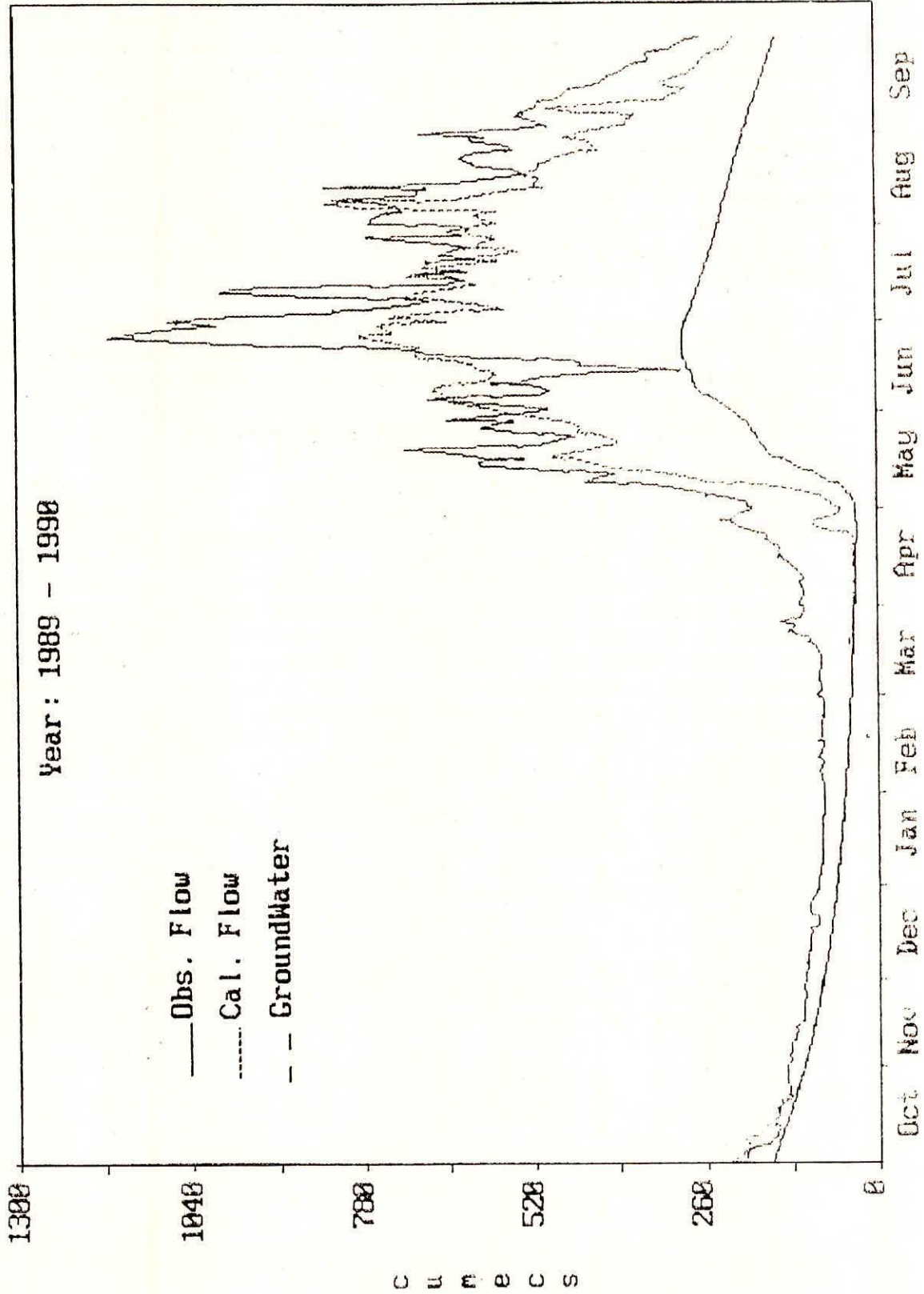


Figure 9(c) Observed and simulated streamflows for the year 1989/90 considering watershed as a single unit



It is can be seen from the results from the Spiti basin alone that simulation accuracy is reasonably high for this basin. The results for the lower sub-basins are not so good, partly because the flow data is less reliable, being based on the differencing up of upstream flows (Table 1). The simulation results presented in Figures 10(a) to (c) should be compared with Figures 12(a) to (c) for the whole basin simulation. The flow in the months of April and May in the year of 1987/88 was underestimated by considering the watershed as a single unit while it was well simulated by the combination of two sub-basins. For the year 1988/89 the simulated flows in the month of June could not match measured flows, which reduced drastically in this month. However, the combination of the two sub-basins followed the pattern of the observed flows. The peak in the end of June and beginning of July for the year 1989/90 was missed when considering the whole watershed as a single unit, but this peak was correctly simulated when using the combination of two sub-basins.

It is evident that the results obtained by combining the separate simulations for the upper and lower sub-basins are superior and this is confirmed by statistical measures of fit such as the Nash-Sutcliffe efficiency ( $R^2$ ) measure as shown in Table-1. The main reason for this improvement is because the two sub-basins are somewhat different hydrologically. The upper sub-basin has less glaciers in comparison to the lower part of the basin, however, it covers a higher elevation range. Other differences may be because of significant differences in the orientation of the major part of the sub-basins. For example, the upper sub-basin has an average south-east orientation with the elevation range from about 2900 m to 7026 m, while the lower sub-basin has, in general, a north-west orientation and covers an elevation range from about 1500 to 4600 m. Therefore, the pattern of precipitation indicates a wide variation in both sub-basins. The precipitation is produced by the same weather system in the whole watershed but the existing topography substantially changes the precipitation. It can be inferred from the patterns of mean monthly precipitation (Figure 3) that Kalpa, although located at a lower elevation in the watershed, receives higher precipitatin in comparison to Namgia and Kaza which are at higher elevations. Such variations may result in errors in simulation when the watershed is considered as a single unit.

A plot of the estimated snowpack water equivalent in millimeters for the year 1988-89 for the Spiti catchment is shown in Figure 13. It can be seen that the snowpack builds up during the winter period, reaching a maximum in March or April. Generally

Figure 10(a) Observed and simulated streamflows for the year 1987/88 for the upper subbasin (Spiti)

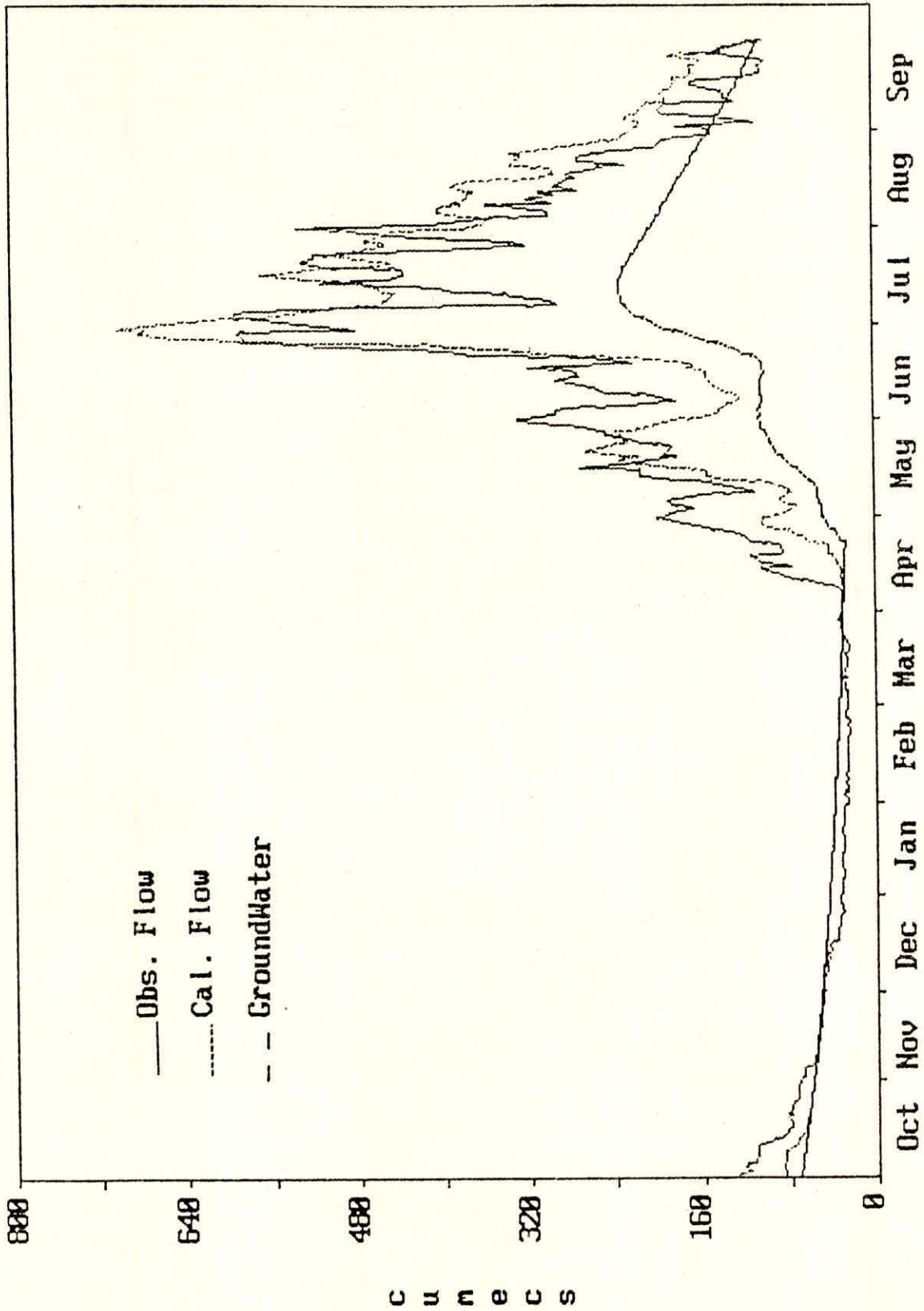


Figure 10(b) Observed and simulated streamflows for the year 1988/89 for the upper subbasin (Spiti)

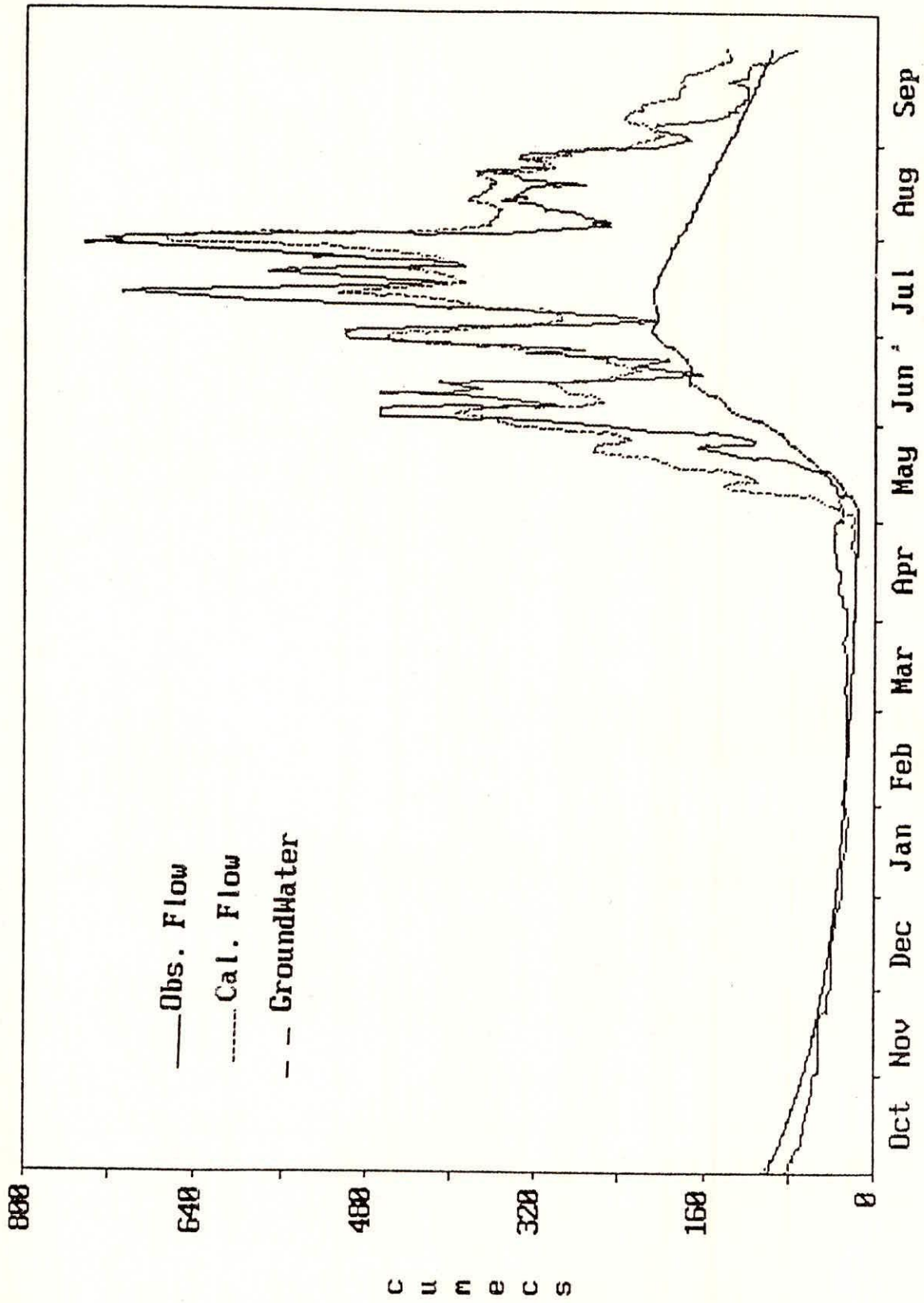


Figure 10(c) Observed and simulated streamflows for the year 1989/90 for the upper subbasin (Spiti)

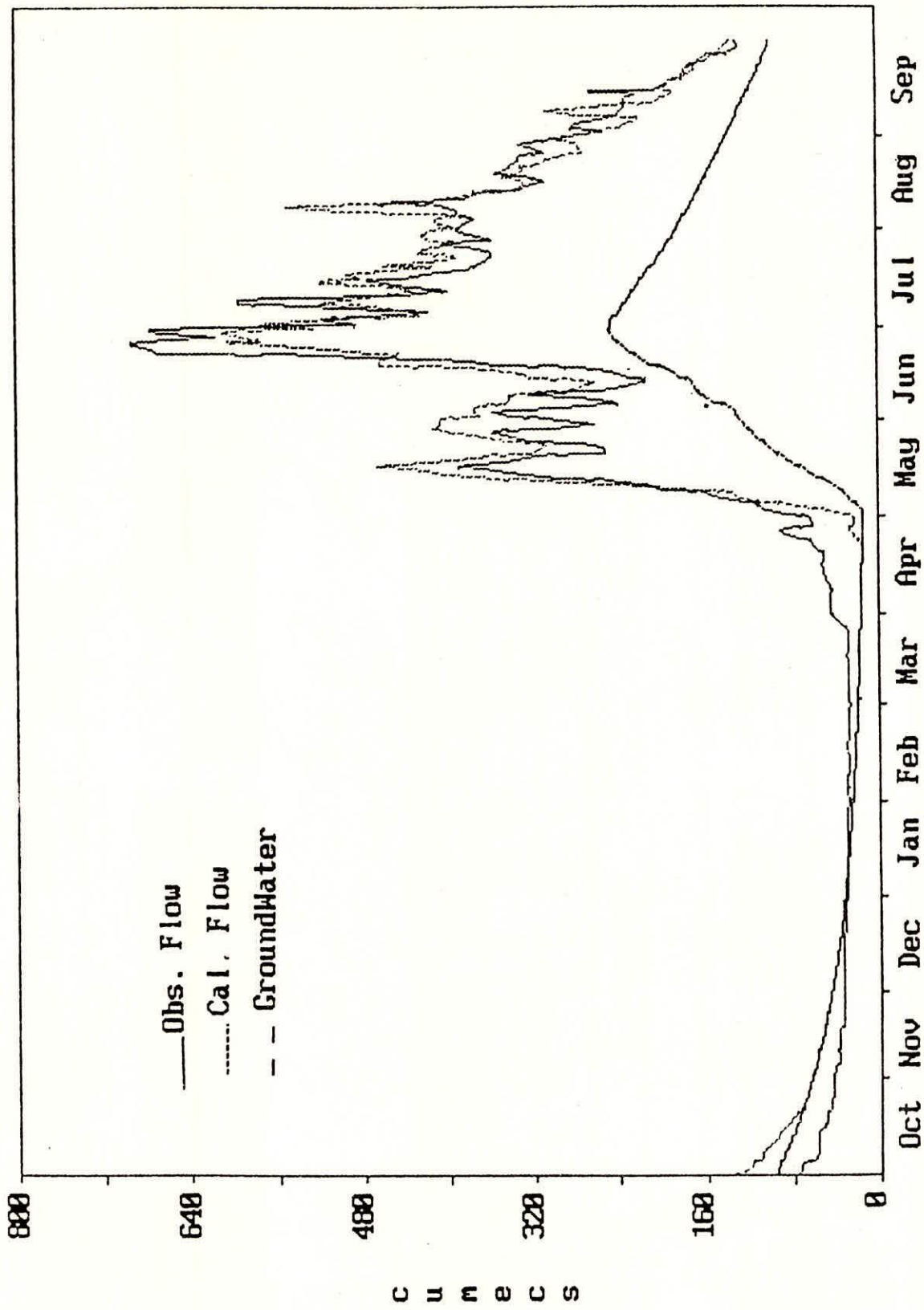


Figure 11(a) Observed and simulated streamflows for the year 1987/88 for the lower subbasin

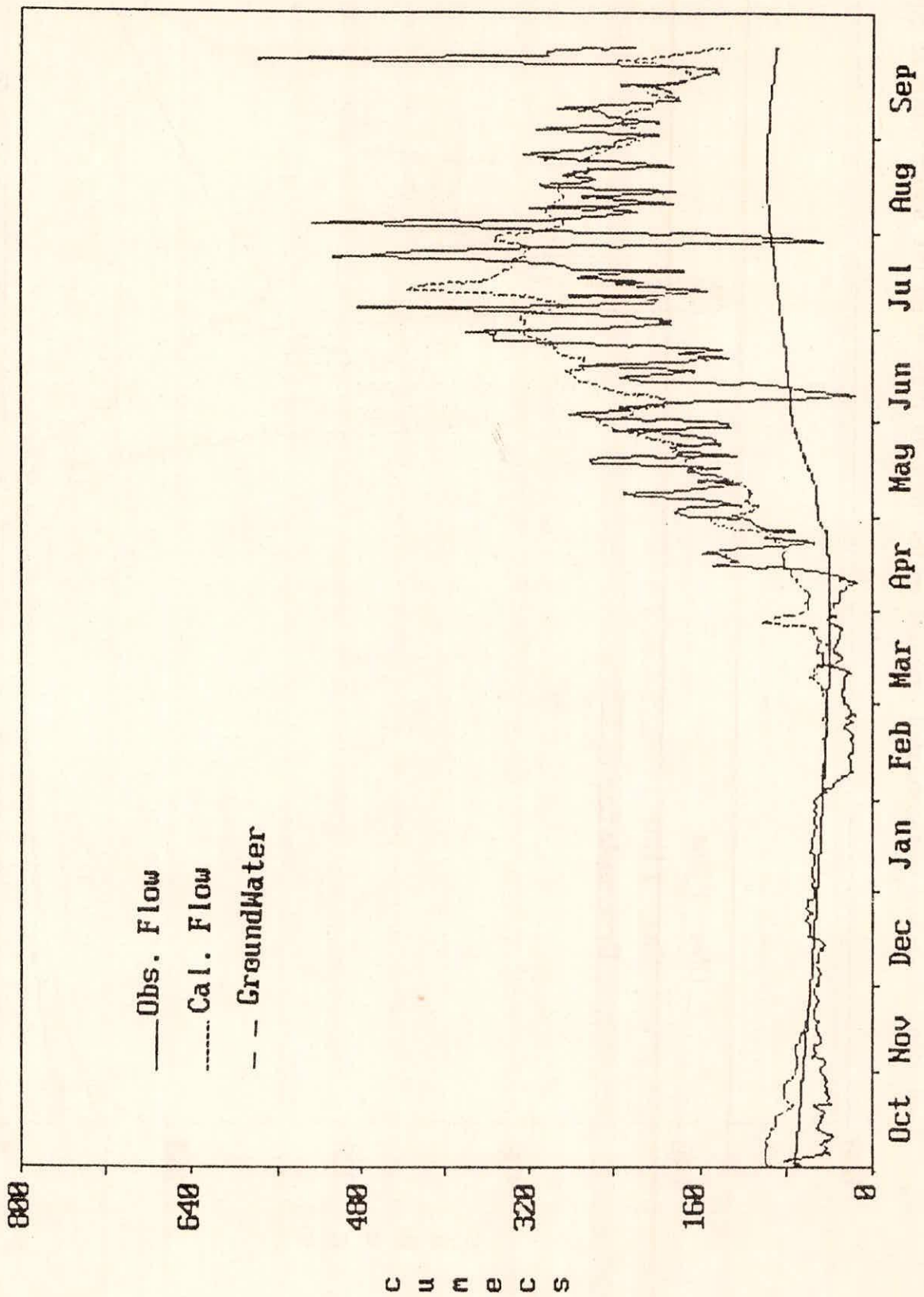




Figure 11(b) Observed and simulated streamflows for the year 1988/89 for the lower subbasin

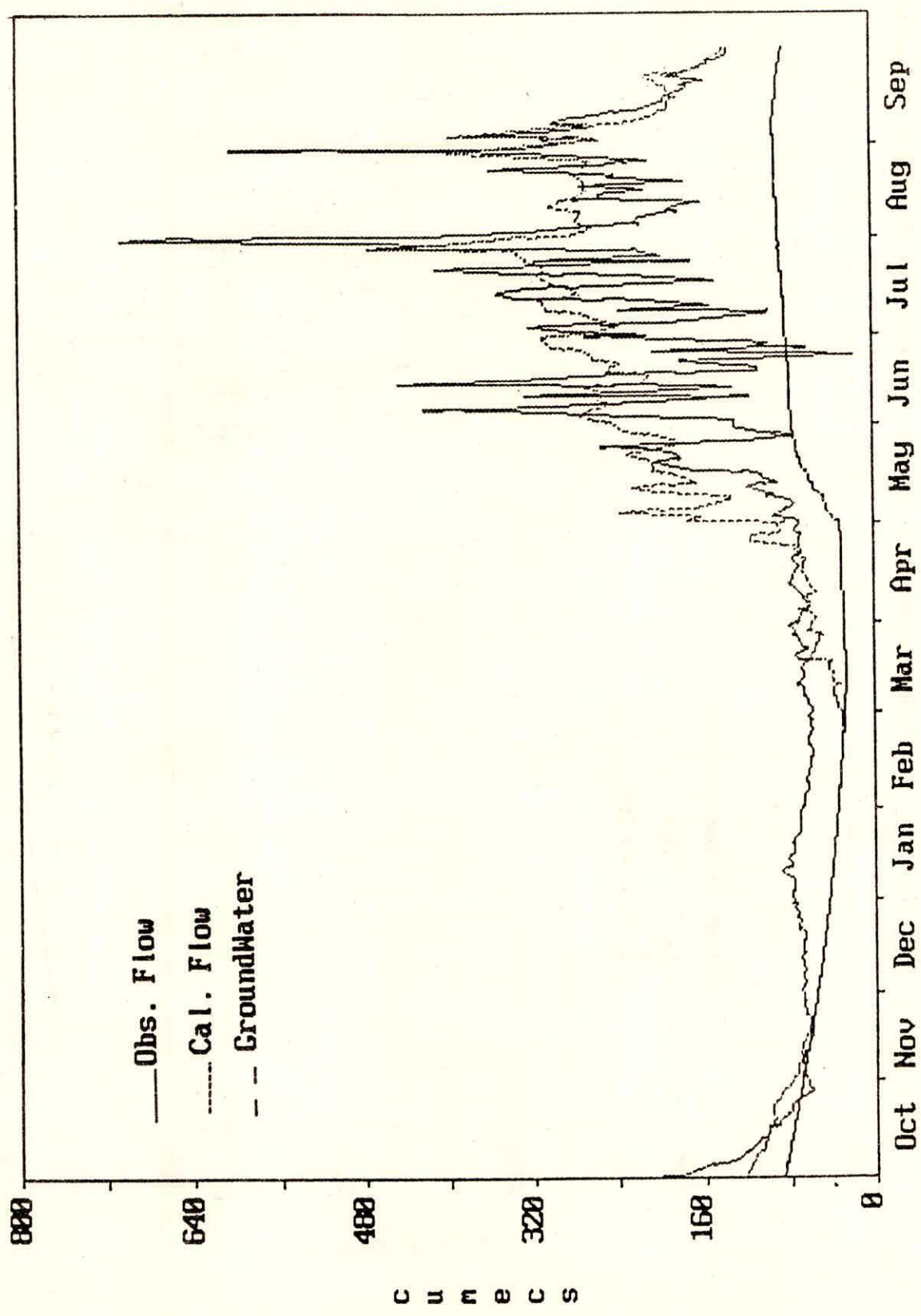


Figure 11(c) Observed and simulated streamflows for the year 1989/90 for the lower subbasin

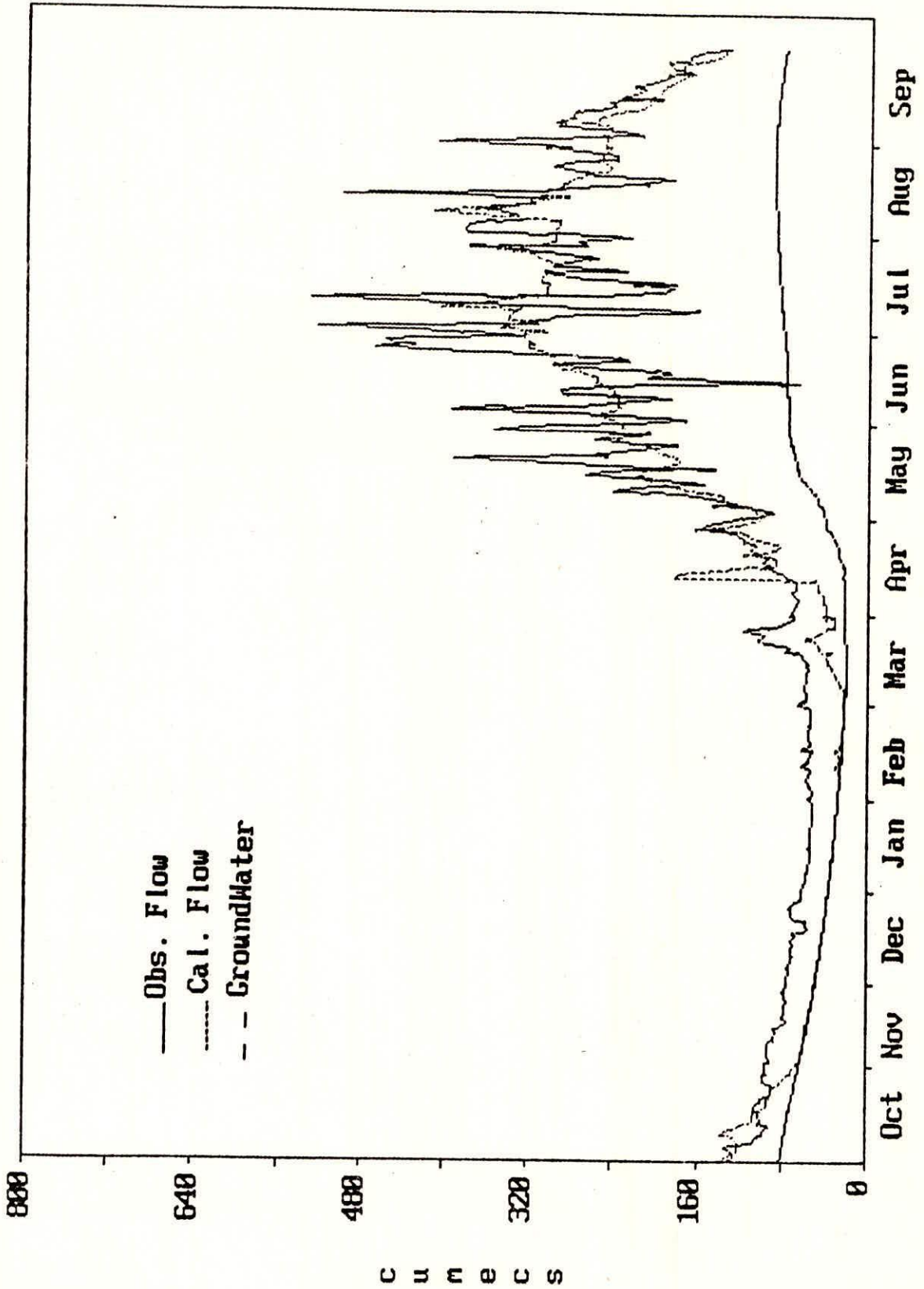


Figure 12(a) Observed and simulated streamflows for the year 1987/88 by splitting watershed into two subbasins and combining the flows.

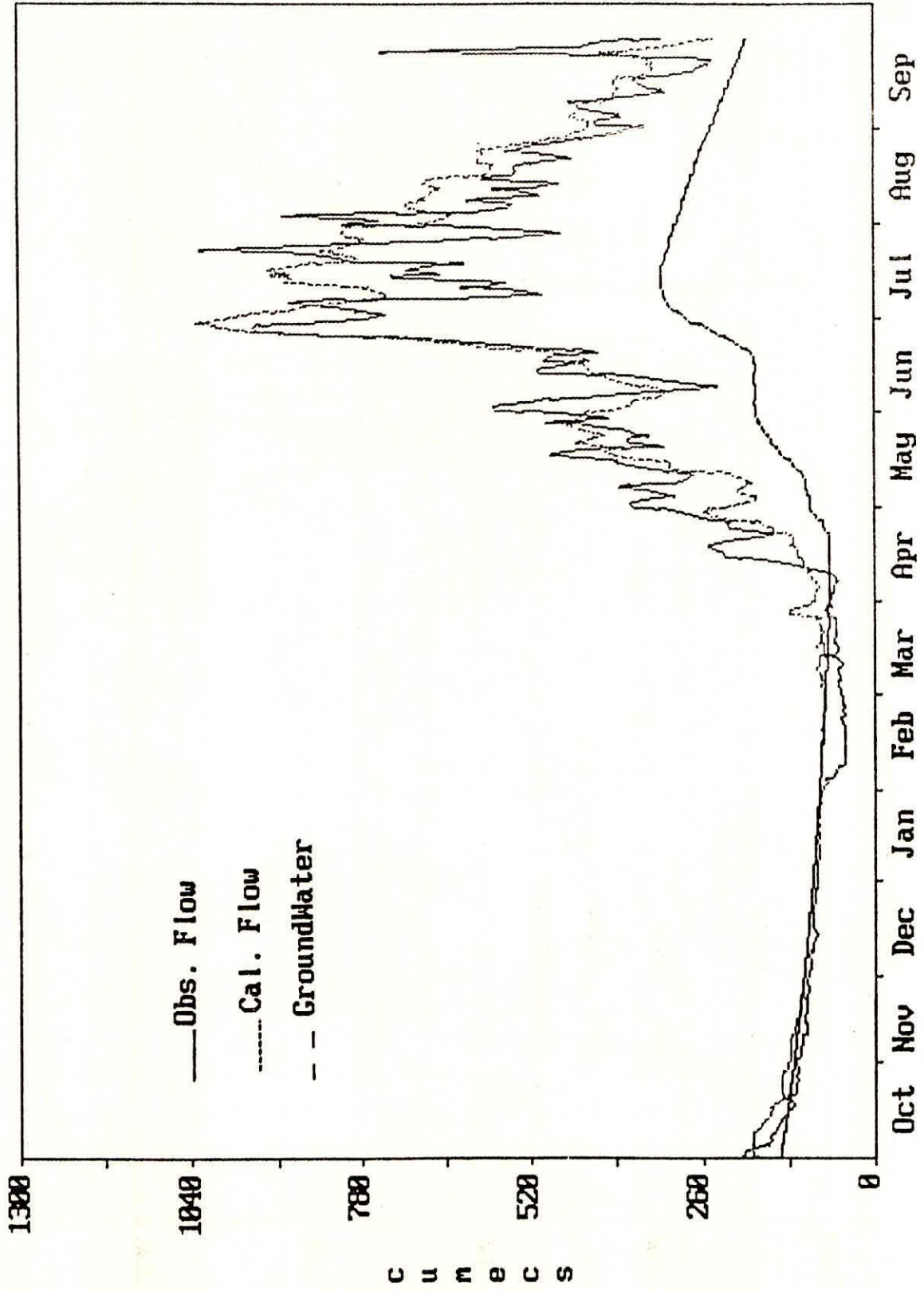


Figure 12(b) Observed and simulated streamflows for the year 1988/89 by splitting watershed into two subbasins and combining the flows

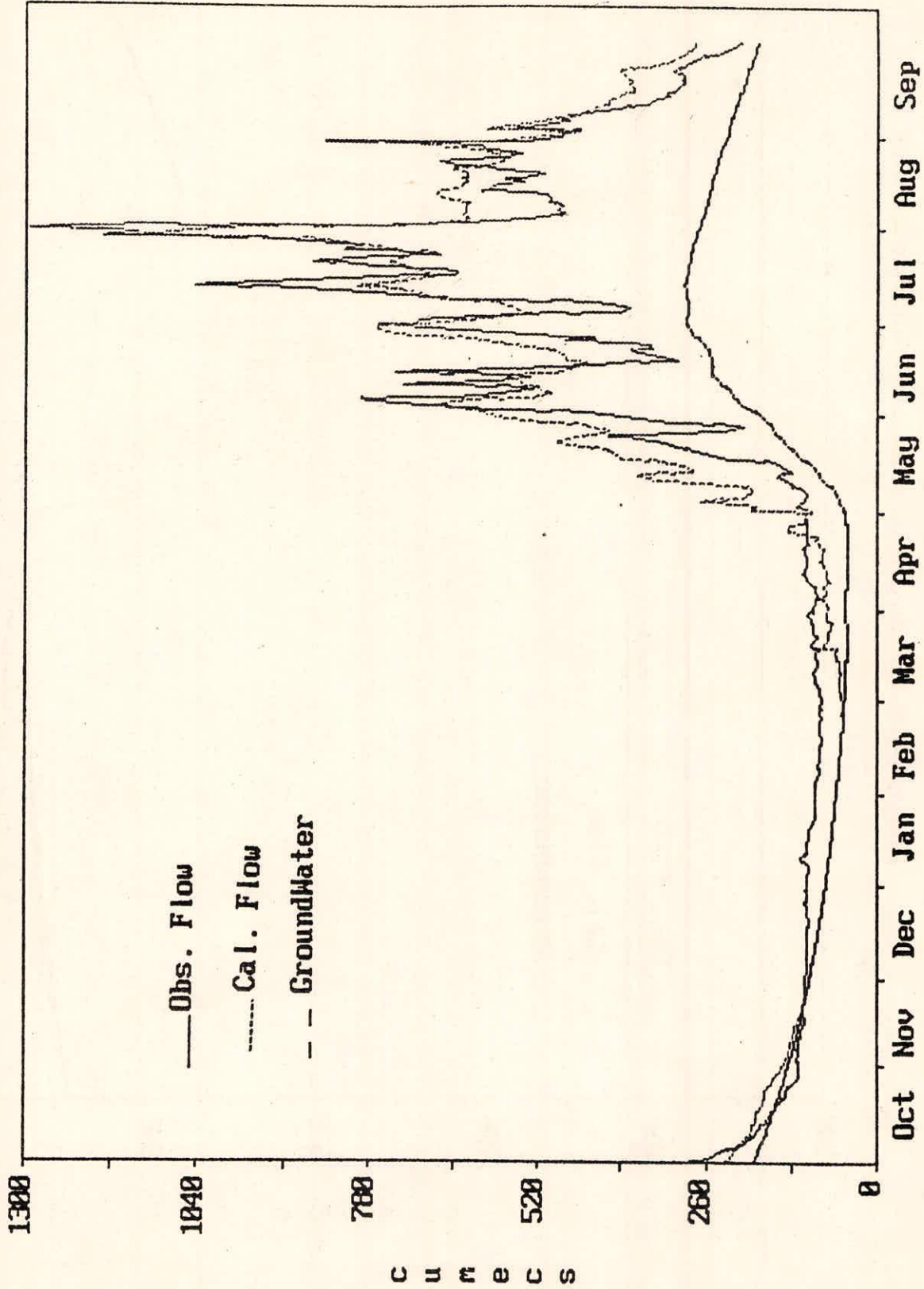


Figure 12(c) Observed and simulated streamflows for the year 1989/90 by splitting watershed into two subbasins and combining the flows

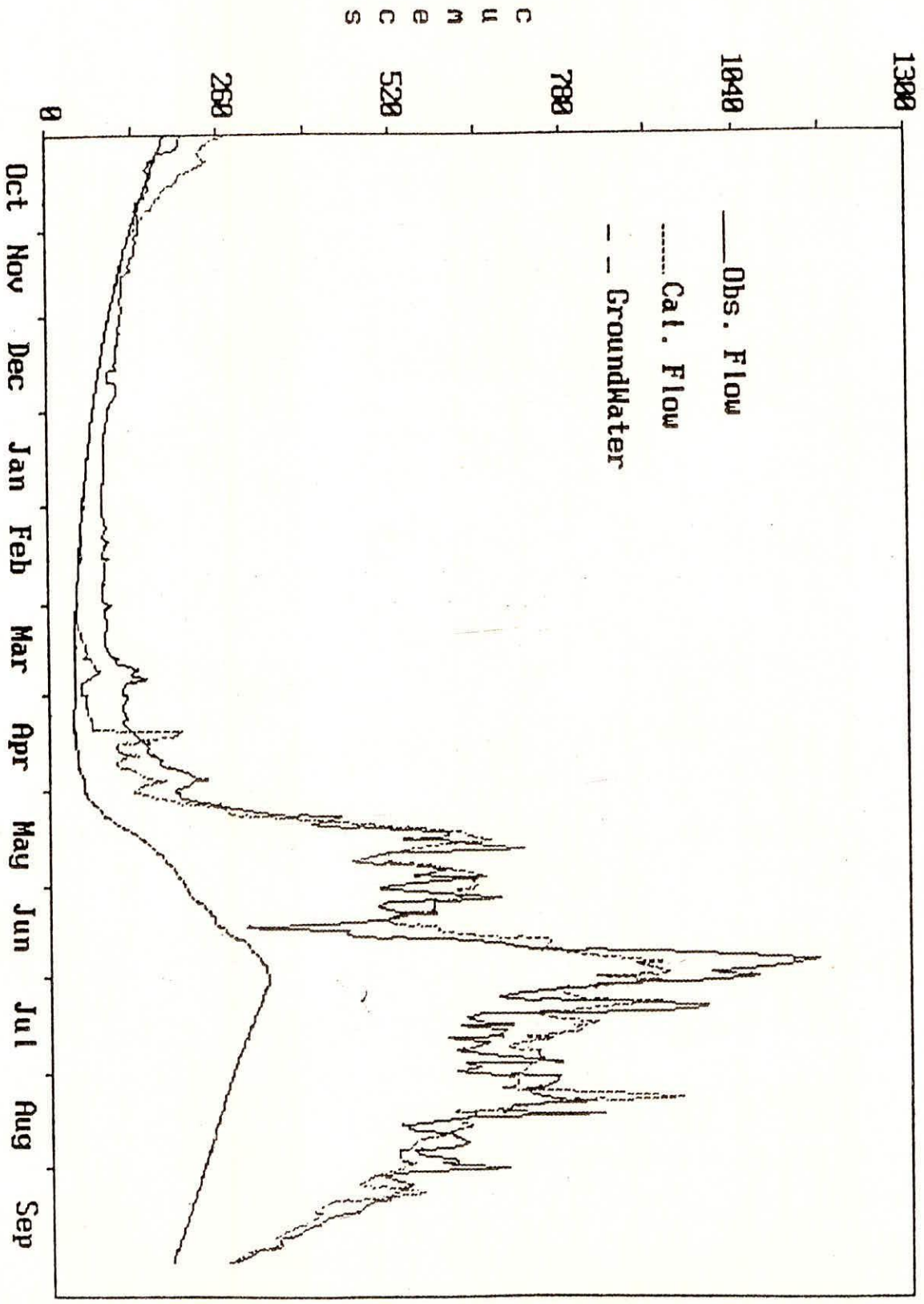
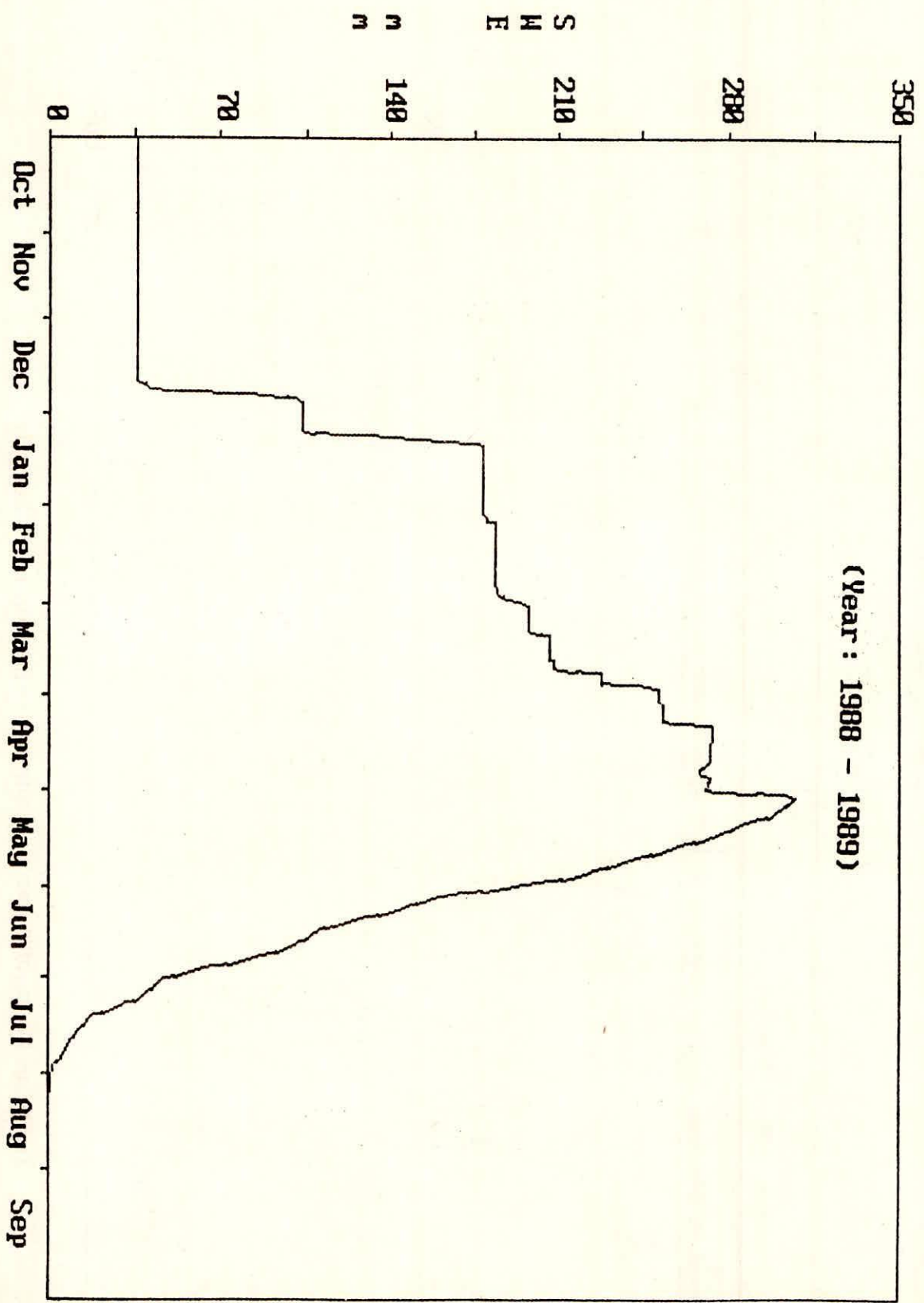


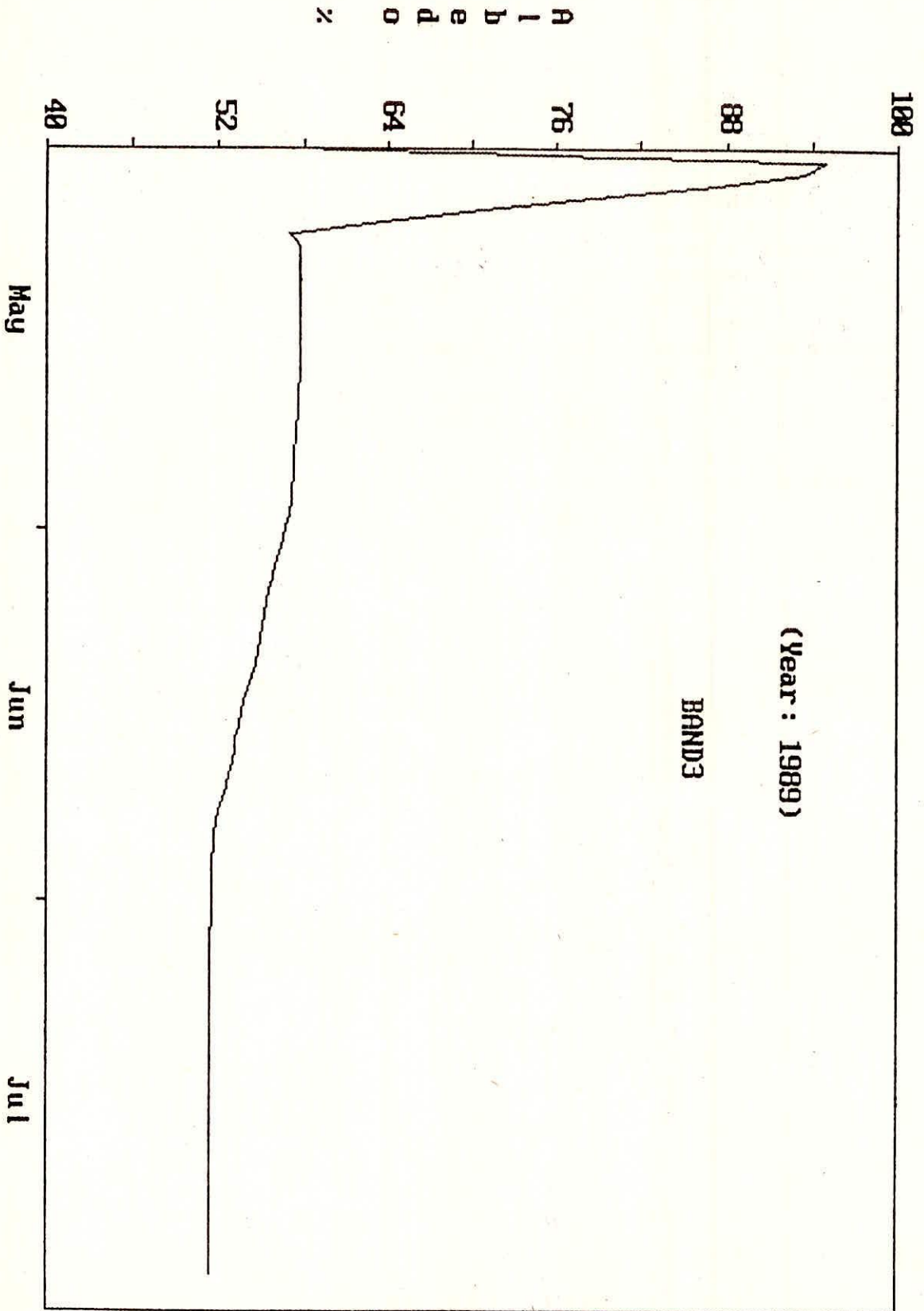
Figure 13: Build-up and depletion of snow water equivalent for the year, 1988-89.



April to July there is melting of the snowpack in response to the high solar radiation and the associated warm air temperatures. The seasonal snowcover is melted by late June or July, and further melt then occurs from the snowfree glaciated areas. This rapid melting is computed from the equations presented earlier and is clearly indicated by the rapid reduction of snow water equivalent.

Figure 14 shows the computed values of the albedo of the snowcover for a particular elevation zone of the Spiti watershed. Can be seen that the winter snowcover has a high albedo, so that only a small fraction of the incoming solar radiation is absorbed by the snowpack. Consequently melt rates are low at the start of the season. As the melt season progress, the snow crystal structure changes by cause of freeze thaw cycling which causes the of the snow to reduce. Figure 14 indicates a gradual reduction in albedo from 0.9 to value of 0.5 or less. Then new snow falls, the albedo increases again to that of new snow, but after more melt occurs, the albedo returns to its previous lower value. This albedo modelling is an important aspect of the estimation of snowmelt because if albedo changes from 0.9 to 0.6 the melt rate will increase by a factor of about four. A snowfree glaciated surface can typically have an albedo of 0.3, so that the melt rate can then be seven times greater than new snow, and twice as high as a snowpack with an albedo of 0.6, which is typical of a moderately aged snowpack.

Figure 14: Changes in albedo with season.





## 6.0 CONCLUSIONS

The high variability in the precipitation, which is one of the characteristics of Himalayan watersheds, makes watershed modelling complex. The snowmelt estimates and observed streamflow are used in combination to determine precipitation gradients and representative factors. These analyses indicate large variation in precipitation at high elevations and emphasize the hydrological importance of these high mountain region which play a significant role in snowmelt and glacier melt runoff. The results confirm that it is reasonable to assume that the mountain precipitation pattern is predictable and falls in a repeatable pattern from year to year. Mountain watershed modelling is possible even one or two reliable data stations are available. If they are situated high enough in the watershed, those can be good indicators of basin precipitation. Valley precipitation is unreliable because no precipitation may be recorded even when considerable precipitation is falling at high elevations.

It is the extent of snowpack and its thaw that principally contribute to the melt water yield. The results indicate that snowmelt and glacier melt can be reliably computed from a simplified energy budget method using daily maximum and minimum temperature as basic input data. The snowmelt and glacier melt are more forecastable than rain because snowpacks are built up during a whole season and measured cumulative precipitation is usually a good statistical representation of snowpack.

The flow estimates for the watershed when split into sub-basins are compared with the results calculated for the same total area treated as single watershed, and this comparison indicates that better results are obtained by calculating each sub-basin separately and then combining the results. This conclusion will be true for simulation of forecasting of streamflows when the individual sub-basins have a different hydrologic behaviour and when the difference in behaviour can be adequately devised by the available meteorological data base.

#### ACKNOWLEDGEMENTS

This study has been carried out as part of a cooperative study between the National Institute of Hydrology, Roorkee, India, and the Civil Engineering Department of the University of British Columbia. Funding for the visit of Dr.Singh from NIH to UBC has been provided by the United nations Development Program. The authors are grateful to Bhakra Beas Management Board (BBMB) for supplying the data for this study.

Table - 1

Model efficiency ( $R^2$ ) for individual sub-basins and total watershed

Watershed	1987/88	1988/89	1989/90
1. Upper sub-basin	0.85	0.89	0.93
2. Lower sub-basin	0.62	0.58	0.79
3. Watershed as a single unit	0.82	0.84	0.84
4. Combination of upper and lower sub-basins	0.88	0.90	0.93

## REFERENCES

1. Agarwal, K.C., Kumar V. and Dass, T. (1983), Snowmelt runoff for subcatchment of Beas basin, Proceedings, First National Symposium on Seasonal Snowcover, 28-30 April, 1983, SASE, Manali, India.
2. Anderson, E.A. (1976), A point energy and mass balance model of a snow cover, NOAA Tech. Report, NWS 19, National Weather Service, U.S.Dept. of Commerce.
3. BBMB (Bhakra Beas Management Board) (1988), Snow hydrology study in India with particular reference to the Satluj and the Beas catchment, Workshop on Snow Hydrology, 23-26 November, 1988, Manali, India.
4. Quick, M.C. (1987), Snowmelt hydrology and applications to runoff forecasting, National Lecture, sponsored by Associate Committee on Hydrology of National Research Council and Hydrotechnical Committee for Canadian Society of Civil Engineers.
5. Quick, M.C. and Pipes, A. (1977), UBC Watershed Model, Hydrological Sciences Bulletin, 22(1), 153-162.
6. Chow, V.T. (1964), Handbook of hydrology, McGraw-Hill, Section 3-7.
7. Ramamoorthi, A.A. (1986), Forecasting snowmelt runoff of Himalayan rivers using NOAA AVHRR imageries since 1980, Proceedings, Hydrologic Applications of Space Technology, IAHS Publication NO.160.
8. Rao, Mohan N. (1983), Some observations on seasonal snowcover, Proceedings First National Symposium on Seasonal Snowcover, 28-30 April, 1983, SASE, Manali, India.
9. S.I.H.P. (Snow and Ice Hydrology project), Annual Reports, Wilfred Laurier University, Waterloo, Ontario, Canada, 1986, 1987, 1988.
10. Singh, P. (1991), Status report on snowmelt modelling studies (unpublished), National Institute of Hydrology, Roorkee, India.
11. Upadhyay, D.S., Chaudhary, J.N. and Katyal, K.N. (1983), An

empirical model for prediction of snowmelt runoff in Satluj,  
Proceedings First National Symposium on Seasonal Snowcover,  
28-30 April, 1983, SASE, Manali, India.

12. U.S. Corps (1952), Hydrometeorological log of the Central Sierra Snow Laboratory, 1948-49, South Pacific Division, Corps of Engineers, U.S. Army, San Francisco.
13. U.S. Corps of Engineers (1955), Lysimeter studies of snowmelt, Snow Investigations, Research Note 25, North Pacific Division, Portland, Oregon, 1-41.